Pharmacological Research 187 (2023) 106552

Contents lists available at ScienceDirect

Pharmacological Research

journal homepage: www.elsevier.com/locate/yphrs

Review

Properties of FDA-approved small molecule protein kinase inhibitors: A 2023 update

Robert Roskoski Jr

Blue Ridge Institute for Medical Research, 3754 Brevard Road, Suite 106, Box 19, Horse Shoe, NC 28742-8814, United States

ARTICLE INFO

Keywords:
Atopic dermatitis
Cholangiocarcinoma
Chronic myelogenous leukemia
Myelofibrosis, Protein kinase inhibitor classification
Treatment-free remission

Chemical compounds studied in this article:
Abrocitinib (PubChem CID: 78323835)
Asciminib (PubChem CID: 72165228)
Dasatinib (PubChem CID: 3062316)
Futibatinib (PubChem CID: 71621331)
Ibrutinib (PubChem CID: 24821094)
Imatinib (PubChem CID: 5291)
Pacritinib (PubChem CID: 46216796)
Ruxolitinib (PubChem CID: 25126798)
Sorafenib (PubChem CID: 216239)
Sunitinib (PubChem CID: 5329102)

ABSTRACT

Owing to the dysregulation of protein kinase activity in many diseases including cancer, this enzyme family has become one of the most important drug targets in the 21st century. There are 72 FDA-approved therapeutic agents that target about two dozen different protein kinases and three of these drugs were approved in 2022. Of the approved drugs, twelve target protein-serine/threonine protein kinases, four are directed against dual specificity protein kinases (MEK1/2), sixteen block nonreceptor protein-tyrosine kinases, and 40 target receptor protein-tyrosine kinases. The data indicate that 62 of these drugs are prescribed for the treatment of neoplasms (57 against solid tumors including breast, lung, and colon, ten against nonsolid tumors such as leukemia, and four against both solid and nonsolid tumors: acalabrutinib, ibrutinib, imatinib, and midostaurin). Four drugs (abrocitinib, baricitinib, tofacitinib, upadacitinib) are used for the treatment of inflammatory diseases (atopic dermatitis, psoriatic arthritis, rheumatoid arthritis, Crohn disease, and ulcerative colitis). Of the 72 approved drugs, eighteen are used in the treatment of multiple diseases. The following three drugs received FDA approval in 2022 for the treatment of these specified diseases: abrocitinib (atopic dermatitis), futibatinib (cholangiocarcinomas), pacritinib (myelofibrosis). All of the FDA-approved drugs are orally effective with the exception of netarsudil, temsirolimus, and trilaciclib. This review summarizes the physicochemical properties of all 72 FDA-approved small molecule protein kinase inhibitors including lipophilic efficiency and ligand efficiency.

1. The importance of therapeutic protein kinase inhibitors

Because of genetic alterations including mutations and translocations as well as overexpression, the dysregulation of protein kinase activity plays a significant role in the pathogenesis of autoimmune, inflammatory, nervous, and cardiovascular diseases as well as a number of malignancies. Consequently, protein kinases are among the most important drug targets in the 21st century [1,2]. Perhaps 25–33% of drug development efforts in the United States and worldwide target these enzymes. The clinical efficacy of imatinib in the treatment of Philadelphia chromosome-positive chronic myelogenous leukemia in 2001 motivated the search for orally bioavailabe therapeutic protein kinase antagonists [3–5]. This remarkable success resulted from the imatinib blockade of the active chimeric BCR-Abl protein-tyrosine kinase, the causative biochemical defect that produces these leukemias.

The repertoire of several thousand protein kinase X-ray crystal structures in the public domain expedite structure-based drug development. Furthermore, additional proprietary structures solved by commercial ventures are in widespread use in the drug development process. Approximately 180 orally bioavailable protein kinase inhibitors are in clinical trials worldwide [6]. A comprehensive catalog of these medicinals, which is regularly updated, can be obtained at www.icoa.fr/pkidb/. There are 72 FDA-approved drugs that target about two dozen different protein kinases (see supplementary material). These protein kinases, however, represent a small fraction of the 518-member protein kinase enzyme family. Additional agents directed against these and other protein kinases are in clinical trials in the United States and across the globe [4–7].

Abbreviations: AS, activation segment; BP, back pocket; C-spine, catalytic spine; CS1, catalytic spine residue 1; CML, chronic myelogenous leukemia; CL, catalytic loop; EGFR, epidermal growth factor receptor; F, front pocket; FGFR, fibroblast growth factor receptor; GK, gatekeeper; GRL, glycine-rich loop; JAK, Janus kinase; KLIFS-3, kinase-ligand interaction fingerprint and structure residue-3; LE, ligand efficiency; LipE, lipophilic efficiency; NSCLC, non-small cell lung cancer; PDGFR, platelet-derived growth factor receptor; PI, phosphatidylinositol; PKA, protein kinase A; PSA, polar surface area; Ro5, Lipinski's rule of five; R-spine, regulatory spine; RS1, regulatory spine residue 1; Sh2, shell residue 2; VEGFR, vascular endothelial growth factor receptor.

E-mail address: rrj@brimr.org.

https://doi.org/10.1016/j.phrs.2022.106552
Received 8 November 2022; Accepted 8 November 2022
Available online 17 November 2022

Manning et al. reported that the human protein kinase lineage contains 478 typical and 40 atypical enzymes [8] including phosphatidylinositol 3-kinase (PI 3-kinase) [5,9]. Protein kinases catalyze the following reaction;.

$MgATP^{1-}$ + protein–O:H → protein–O:PO_3^{2-} + MgADP + H^+.

Based upon the identity of the protein–OH groups, these catalysts are divided into, protein-tyrosine kinases (90 members), protein-tyrosine kinase–like enzymes (43), and protein-serine/threonine kinases (385). The protein-tyrosine kinase lineage consists of both transmembrane receptor (58) and intracellular nonreceptor (32) proteins. Furthermore, the protein kinase lineage includes a small group of intracellular enzymes such as MEK1/2 that catalyze the phosphorylation of both tyrosine and then threonine residues within the activation segment of their target protein kinases; because of this unique action, MEK1/2 and related enzymes are called dual specificity protein kinases. Another indication of the importance of the protein kinase family is the estimate that about one in every 40 human genes (518 protein kinase genes out of an estimated 20,000 human protein-encoding genes) codes for a protein kinase. Protein kinases therefore constitute about 2.5% of the human genome. Another indication of the importance of protein kinases as drug targets is the work of Manning et al. that suggests that 244 protein kinases map to cancer amplicons and other disease loci [8]. Consequently, as additional research on the pathogenesis of various diseases is performed, it is highly likely that there will be a notable increase in the number of protein kinase therapeutic targets.

The US FDA has approved 72 small molecule therapeutic protein kinase inhibitors as of 24 November 2022 (see supplementary material), nearly all of which are orally effective with the exceptions of netarsudil (an eye drop) and temsirolimus and trilaciclib (which are given intravenously). Ruxolitinib is an orally bioavailable JAK1/2 therapeutic protein kinase inhibitor that was approved for the treatment of polycythemia vera and myelofibrosis in 2011. This agent is topically active as a cream and was approved in 2021 for the treatment of atopic dermatitis. Of the 72 approved drugs, forty target receptor protein-tyrosine kinases, sixteen block nonreceptor protein-tyrosine kinases, twelve inhibit protein-serine/threonine protein kinases, and four are directed against dual specificity protein kinases (MEK1/2) (Table 1). The data indicate that 62 of these medicinals are approved for the management of neoplasms (50 against solid tumors such as lung, colon, and breast, eight against nonsolid tumors such as leukemia, and four against both types of tumors: midostaurin, ibrutinib, imatinib, and acalabrutinib).

More than two dozen of the approved drugs are multikinase antagonists. Because the specificity of many of the protein kinase inhibitors has not been examined, it is probable that many more of the approved drugs are multikinase inhibitors. The simultaneous blockade of several protein kinases has potential advantages and disadvantages. For example, the therapeutic effectiveness of multikinase antagonists may be related to the blockade of two or more targets. Cabozantinib and sunitinib, for instance, have potent off-target activity against the Axl receptor protein-tyrosine kinase and this property may add to their clinical efficacy [14]. In contrast, the inhibition of off-target kinases may elicit unwanted side effects. Accordingly, we have the dilemma of whether a magic shotgun should be preferred to Paul Ehrlich's magic bullet [15].

Eleven of the FDA-approved protein kinase inhibitors are prescribed for the treatment of nonneoplastic diseases. For example, (i) netarsudil is employed for the treatment of glaucoma, (ii) ruxolitinib, ibrutinib, and belumosudil are prescribed for the management of graft vs. host disease, (iii) nintedanib is used for the treatment of idiopathic pulmonary fibrosis, (iv) fostamatinib is prescribed for the management of chronic immune thrombocytopenia, (v) baricitinib, tofacitinib, and upadacitinib are employed for the treatment of rheumatoid arthritis, (vi) ruxolitinib, upadacitinib, and the newly approved abrocitinib are prescribed for the management of atopic dermatitis, (vii) tofacitinib is used for the treatment of psoriatic arthritis, rheumatoid arthritis, and ulcerative colitis, and (viii) upadacitinib is prescribed for the treatment of psoriatic arthritis, rheumatoid arthritis, and atopic dermatitis [10–13]. Moreover, sirolimus and ibrutinib are approved therapeutics for both neoplastic and nonneoplastic diseases.

Seven of the FDA-approved kinase inhibitors form covalent bonds with their target enzymes and they are accordingly classified as TCIs (targeted covalent inhibitors) [16]. These agents include acalabrutinib (inhibiting BTK in mantle cell lymphoma), dacomitinib (inhibiting mutant *EGFR* in NSCLC), osimertinib (blocking *EGFR T970M* mutants in NSCLC), afatinib (targeting EGFR in NSCLC), neratinib (targeting ErbB2 in HER2-positive breast cancer), zanubrutinib (targeting BTK in mantle cell lymphoma), and ibrutinib (blocking BTK in chronic lymphocytic leukemia, mantle cell lymphoma, marginal zone lymphoma, chronic graft vs. host disease, and Waldenström macroglobulinemia). The closely related EGFR and ErbB4 of the ErbB1/2/3/4 epidermal growth factor receptor family are the most common protein kinases bearing mutations in all cancers [3]. For a summary of the characteristics of small molecule protein kinase blockers that were approved by the FDA prior to 2022, see Refs. [10–13].

Of the 72 FDA-approved protein kinase inhibitors, nineteen are prescribed for the treatment of more than one disease. For example, imatinib is approved for the treatment of eight distinct maladies (Table 1). This agent inhibits the nonreceptor protein-tyrosine kinase Abl (and the BCR-Abl chimera – responsible for the pathogenesis of chronic myelogenous leukemia), Abl2, PDGFRα/β, Kit (the stem cell factor receptor), and epithelial discoidin domain-containing receptor-1 (DDR1) and receptor-2 (DDR2). DDR1/2, which are activated by collagen, participate in cell migration, proliferation, differentiation, and remodeling the extracellular matrix. Imatinib is FDA-approved for (i) the first-line treatment of Philadelphia chromosome-positive chronic myelogenous leukemia, (ii) myelodysplastic/myeloproliferative diseases with *PDGFR* gene-rearrangements, (iii) *KIT* mutation-positive gastrointestinal stromal tumors, (iv) dermatofibrosarcoma protuberans, (v) acute lymphoblastic leukemia, (vi) chronic eosinophilic leukemia, (vii) hypereosinophilic syndrome, and (viii) as a second-line treatment for aggressive systemic mastocytosis without the KIT^{D816V} mutation [2,10]. Imatinib is used off-label for the treatment of chronic myelogenous leukemia following allogeneic stem cell transplantation, advanced *KIT*-mutant melanomas, chordomas, and desmoid tumors. Imatinib is thus a broad-spectrum inhibitor.

2. Protein kinase structure and mechanism

2.1. Primary, secondary, and tertiary structures

The newly approved drugs described in this review interact with (i) the nonreceptor protein tyrosine kinases JAK1, JAK2, and chimeric BCR-Abl and (ii) the receptor protein-tyrosine kinases FGFR1/2/3/4 so that the following description is generic. As described initially for PKA (protein kinase A) by Knighton et al., protein kinases have a small N-terminal lobe and large C-terminal lobe (Fig. 1) [17]. The N-terminal lobe is made up of a five-stranded antiparallel β-sheet (β1–β5) and an αC-helix that occurs in active and inactive orientations [18,19]. This lobe contains a glycine-rich loop (GRL), sometimes called the P-loop (for the ATP phosphates), which connects the small lobe β1- and β2-strands; the loop consists of GxGxΦG where the Φ denotes a hydrophobic residue. A valine residue that is two residues after the G-rich loop makes hydrophobic contact with the adenine portion of ATP as well as numerous small molecule protein kinase blockers. Protein kinases possess an AxK sequence within the β3-strand and a conserved glutamate near the middle of the αC-helix. A salt bridge links the positively charged β3-strand lysine (K) and the negatively charged αC-glutamate (E) in catalytically competent protein kinases and such structures correspond to an "αC_{in}" conformation (Fig. 1A). The αC_{in} architecture is necessary, but not sufficient, for the manifestation of full enzyme activity. Moreover, the absence of this salt bridge demonstrates that the

Table 1
FDA-approved small molecule protein kinase inhibitors, their protein kinase targets, and therapeutic indications[a].

Drug	Code	Company	Trade name	Year approved	Primary targets[b]	Therapeutic indications[c]
Abemaciclib	LY2835219	Lilly	Verzenio	2017	CDK4/6	Combination therapy with (i) an aromatase inhibitor or with (ii) fulvestrant or (iii) as a monotherapy for breast cancer
Abrocitinib	PF-04965842	Pfizer	Cibinqo	2022	JAK1	Atopic dermatitis
Acalabrutinib	ACP-196	Acerta Pharma	Calquence	2017	BTK	Mantle cell lymphomas, CLL, SLL
Afatinib	BIBW 2992	Boehringer Ingelheim	Tovok	2013	ErbB1/2/4	NSCLC, squamous NSCLC
Alectinib	CH5424802	Roche	Alecensa	2015	ALK, RET	ALK-positive NSCLC
Asciminib	ABL001	Novartis	Scemblix	2021	BCR-Abl	Ph^+ CML
Avapritinib	BLU285	Blueprint Medicines	Ayvakit	2020	PDGFRα	GIST with *PDGFRα* exon 18 mutations
Axitinib	AG-013736	Pfizer	Inlyta	2012	VEGFR1/2/3	RCC
Baricitinib	LY 3009104	Lilly	Olumiant	2018	JAK1/2	Rheumatoid arthritis
Belumosudil	KD025	Kadmon Pharma	Rezurock	2021	ROCK2	Graft vs. host disease
Binimetinib	MEK162	Array BioPharma	Mektovi	2018	MEK1/2	Combination therapy with encorafenib for $BRAF^{V600E/K}$ melanomas
Bosutinib	SKI-606	Pfizer	Bosulif	2012	BCR-Abl	Ph^+ CML
Brigatinib	AP 26113	Ariad Pharm	Alunbrig	2017	ALK	ALK-positive NSCLC
Cabozantinib	BMS-907351	Exelixis	Cometriq	2012	RET, VEGFR2	Medullary thyroid cancer, RCC, HCC
Capmatinib	INC-280	Novartis	Tabrecta	2020	MET	NSCLC with MET exon 14 skipping
Ceritinib	LDK378	Novartis	Zykadia	2014	ALK	ALK-positive NSCLC resistant to crizotinib
Cobimetinib	GDC-0973	Genentech	Cotellic	2015	MEK1/2	$BRAF^{V600E/K}$ melanomas in combination with vemurafenib
Crizotinib	PF 2341066	Pfizer	Xalkori	2011	ALK, ROS1	ALK or ROS1-postive NSCLC, inflammatory myofibroblastic tumors, anaplastic large cell lymphoma
Dabrafenib	GSK2118436	GSK	Tafinlar	2013	B-Raf	$BRAF^{V600E/K}$ melanomas, $BRAF^{V600E}$ NSCLC, $BRAF^{V600E}$ anaplastic thyroid cancers
Dacomitinib	PF-00299804	Pfizer	Visimpro	2018	EGFR	*EGFR*-mutant NSCLC
Dasatinib	BMS-354825	Bristol Myers Squibb	Sprycell	2006	BCR-Abl	Ph^+ CML or ALL
Encorafenib	LGX818	Array BioPharma	Braftovi	2018	B-Raf	Combination therapy with binimetinib for $BRAF^{V600E/K}$ melanomas
Entrectinib	RXDX-101	Ignyta, Inc.	Ignyta	2019	TRKA/B/C, ROS1	Solid tumors with NTRK fusion proteins, ROS1-positive NSCLC
Erdafitinib	JNJ-42756493	Jansen Pharm	Balversa	2019	FGFR1/2/3/4	Urothelial bladder cancer
Erlotinib	OSI-774	Genentech	Tarceva	2004	EGFR	NSCLC, pancreatic cancer
Everolimus	RAD001	Novartis	Afinitor	2009	FKBP12/mTOR	HER2-negative breast cancer, pancreatic neuroendocrine tumors, RCC, angiomyolipomas, subependymal giant cell astrocytomas
Fedratinib	TG101348	Celgene	Inrebic	2019	JAK2	Myelofibrosis
Fostamatinib	R788	Rigel Pharma.	Tavalisse	2018	Syk	Chronic immune thrombocytopenia
Futibatinib	TAS_120	Tiaho Pharma	Lytgobi	2022	FGFR2	Bile duct cancers (cholangiocarcinomas) with FGFR2 fusions or other rearrangements
Gefitinib	ZD1839	AstraZeneca	Iressa	2003	EGFR	NSCLC with exon 19 deletions or exon 21 substitutions
Gilteritinib	ASP2215	Astellas Pharma	Xospata	2018	Flt3	AML with *FLT3* mutations
Ibrutinib	PCI-32765	Johnson & Johnson	Imbruvica	2013	BTK	CLL, mantle cell lymphoma, marginal zone lymphoma, graft vs. host disease
Imatinib	STI571	Novartis	Gleevec	2001	BCR-Abl	Ph^+ CML or ALL, aggressive systemic mastocytosis, chronic eosinophilic leukemia, dermatofibrosarcoma protuberans, hypereosinophilic syndrome, GIST, myelodysplastic/myeloproliferative disease
Infigratinib	BGJ 398	QED Therapeutics	Truseltiq	2021	FGFR2	Cholangiocarcinomas with FGFR2 fusions or other rearrangements
Lapatinib	GW572016	GSK	Tykerb	2007	EGFR, ErbB2/HER2	HER2-positive breast cancer
Larotrectinib	LOXO-101	Bayer	Vitrakvi	2018	TRKA/B/C	Solid tumors with NTRK fusion proteins
Lenvatinib	AK175809	Easai Co.	Lenvima	2015	VEGFR, RET	Differentiated thyroid cancer
Lorlatinib	PF-06463922	Pfizer	Lorbrena	2018	ALK	ALK-positive NSCLC
Midostaurin	CPG 41251	Novartis	Rydapt	2017	Flt3	AML, mastocytosis, mast cell leukemia
Mobocertinib	TAK-788	Takeda Pharm.	Exkivity	2021	EGFR	NSCLC with *EGFR*-positive exon 20 insertions
Neratinib	HKI-272	Puma Biotech	Nerlynx	2017	ErbB2/HER2	HER2-positive breast cancer
Netarsudil	AR11324	Aerie Pharma	Rhopressa	2018	ROCK1/2	Glaucoma
Nilotinib	AMN107	Novartis	Tasigna	2007	BCR-Abl	Ph^+ CML
Nintedanib	BIBF-1120	Boehringer Ingelheim	Vargatef	2014	FGFR1/2/3	Idiopathic pulmonary fibrosis
Osimertinib	AZD-9292	AstraZeneca	Tagrisso	2015	EGFR T970M	NSCLC with exon 19 deletions or exon 21 substitutions
Pacritinib	SB1518	CTI BioPharma	Vonjo	2022	JAK2	Myelofibrosis
Palbociclib	PD-0332991	Parke-Davis	Ibrance	2015	CDK4/6	Estrogen receptor- and HER2-positive breast cancers

(*continued on next page*)

Table 1 (*continued*)

Drug	Code	Company	Trade name	Year approved	Primary targets[b]	Therapeutic indications[c]
Pazopanib	GW786034	GSK	Votrient	2009	VEGFR1/2/3	RCC, soft tissue sarcomas
Pemigatinib	INCB054828	Incyte Corp.	Pemazyre	2020	FGFR2	Cholangiocarcinoma with FGFR2 fusions or other rearrangements
Pexidartinib	PLX3397	Plexxikon Inc	Turalio	2019	CSF1R	Tenosynovial giant cell tumors
Ponatinib	AP 24534	Ariad Pharm	Iclusig	2012	BCR-Abl	Ph^+ CML or ALL
Pralsetinib	Blu-667	Blueprint Medicines	Gavreto	2020	RET	RET-fusion (i) NSCLC, (ii) medullary thyroid cancer, (iii) differentiated thyroid cancer
Regorafenib	BAY 73–4506	Bayer	Stivarga	2012	VEGFR1/2/3	Colorectal cancer, GIST, HCC
R406 active metabolite of fostamatinib		Rigel Pharma.		2018	Syk	Chronic immune thrombocytopenia
Ribociclib	LEE011	Novartis	Kisqali	2017	CDK4/6	Combination therapy with an aromatase inhibitor for breast cancer
Ripretinib	DCC-2618	Deciphera Pharma.	Qinlock	2020	Kit, PDGFRα	Fourth-line treatment for GIST
Ruxolitinib	INCB-018424	Incyte Corp.	Jakafi	2011	JAK1/2/3, Tyk	Myelofibrosis, polycythemia vera, atopic dermatitis, graft vs. host disease
Selpercatinib	CEGM9YBNG	Lilly	Retevmo	2020	RET	RET fusion NSCLC and thyroid cancers and *RET* mutant medullary thyroid cancer
Selumetinib	AZD6224	AstraZeneca	Koselugo	2020	MEK1/2	Neurofibromatosis type I
Sirolimus	AY 22989	Wyeth, LLC	Rapamycin	1999	FKBP12/mTOR	Kidney transplants, lymphangioleiomyomatosis
Sorafenib	BAY 43–9006	Bayer	Nexavar	2005	VEGFR1/2/3	HCC, RCC, differentiated thyroid cancer
Sunitinib	SU11248	Pfizer	Sutent	2006	VEGFR2	GIST, pancreatic neuroendocrine tumors, RCC
Temsirolimus	CCI-779	Wyeth, LLC	Torisel	2007	FKBP12/mTOR	RCC
Tepotinib	EMD 1214063	EMD Serono Inc.	Tepmetko	2021	MET	NSCLC with *MET* mutations
Tivozanib	AV951	AVEO Pharma	Fotvida	2021	VEGFR2	Third-line treatment of RCC
Tofacitinib	CP-690550	Pfizer	Tasocitinib	2012	JAK3	Rheumatoid arthritis, psoriatic arthritis, ulcerative colitis
Trametinib	GSK1120212	GSK	Mekinist	2013	MEK1/2	$BRAF^{V600E/K}$ melanoma, $BRAF^{V600E}$ NSCLC
Trilaciclib	G1T28	G1 Therapeutics	Cosela	2021	CDK4/6	Chemotherapy-induced myelosuppression
Tucatinib	ONT-380	Seattle Genetics	Tukysa	2020	ErbB2/HER2	Combination second-line treatment for HER2-positive breast cancer
Upadacitinib	ABT-494	AbbVie	Rinvoq	2019	JAK1	Rheumatoid arthritis, psoriatic arthritis, atopic dermatitis
Vandetanib	ZD6474	Sanofi	Zactima	2011	VEGFR2	Medullary thyroid cancer
Vemurafenib	PLX-4032	Genentech	Zelboraf	2011	B-Raf	$BRAF^{V600E}$ melanomas, Erdheim-Chester disease
Zanubrutinib	BGB3111	BeiGene	Brukinsa	2019	BTK	Mantle cell lymphomas

[a] Drugs not previously reviewed in Refs. [10–13] are given in **bold** type.
[b] Although many of these drugs are multikinase inhibitors, only the primary therapeutic targets are given here.
[c] ALL, acute lymphoblastic leukemias; AML, acute myelogenous leukemias; CLL, chronic lymphocytic leukemias; CML, chronic myelogenous leukemias; ErbB2/HER2, human epidermal growth factor receptor-2; GIST, gastrointestinal stromal tumors; HCC, hepatocellular carcinomas; NSCLC, non-small cell lung cancers; Ph^+, Philadelphia chromosome positive; RCC, renal cell carcinomas; SLL, small lymphocytic leukemias.

enzyme is catalytically inactive and the corresponding structure corresponds to the "αC_{out}" conformation (Fig. 1C). The conversion of the αC_{out} to the αC_{in} conformation is required for catalytic activity.

The large lobe is mainly α-helical with eight conserved helices (αD–αI, αEF1, αEF2) [20]. The carboxyterminal lobe of catalytically active protein kinases also contains four short β-strands (β6–β9) (Fig. 1 A). The second residue of the β7-strand is the floor of the adenine binding pocket and this residue interacts hydrophobically with all known ATP-competitive protein kinase inhibitors [21]. The carboxyterminal lobe contains a catalytic loop (CL) that mediates the transfer of the γ-phosphoryl group from ATP to the peptide/protein substrates. The C-terminal lobe also positions the peptide/protein substrate into the active site to enable catalysis.

Hanks and Hunter described 12 subdomains (I–VIa, VIb–XI) that make up the working components of protein kinases [22]. A K/E/D/D (Lys/Glu/Asp/Asp) tetrad plays an essential role in the enzymatic activity of all protein kinases. The *K* of the tetrad is the β3-strand lysine that forms salt bridges with the (i) αC-glutamate to form the αC_{in} structure and the (ii) α-phosphate and (iii) β-phosphate of ATP (not shown). Residues within the kinase activation segment place the phosphorylatable substrate into the active site. Moreover, the HRD-aspartate of the catalytic-loop (the first *D* of the K/E/*D*/D tetrad) functions as a Lowry-Brönsted base (proton acceptor). Madhusudan et al. suggested that the HRD-aspartate of the catalytic loop abstracts the proton from the protein substrate –OH [23]. Furthermore, Zhou and Adams hypothesized that the HRD-aspartate positions the protein substrate hydroxyl group to promote an in-line nucleophilic attack of the oxygen with the γ-phosphate of ATP [24]. See Ref. [25] for an inclusive summary of protein kinase enzymology and see Table 2 for a list of the important residues in protein kinases considered in this article.

The second *D* of the K/E/D/*D* tetrad is the first residue of the protein-substrate-binding activation segment. This component of all protein kinases starts with DFG and ends with APE or a similar triad such a PPE. Activation segments, which are about 35–40 residues long, are important structural and regulatory components of all protein kinases [26]. An $HRD(x)_4N$ signature constitutes the catalytic loop of active protein kinases. The primary structure of the activation segment occurs C-terminal to the catalytic loop. Two Mg^{2+} ions – $Mg^{2+}(1)$ and $Mg^{2+}(2)$ – are required for the activity of most, but not all, protein kinases. $Mg^{2+}(1)$ interacts with the activation segment DFG-D and $Mg^{2+}(2)$ interacts with the terminal catalytic loop asparagine (not shown).

The amino acid sequence and length of the middle portion of the activation segment vary greatly among the members of the protein kinase superfamily [2]. The activation segment of nearly all members of this superfamily contains one or more phosphorylatable residues. Furthermore, activation segment phosphorylation is required for the

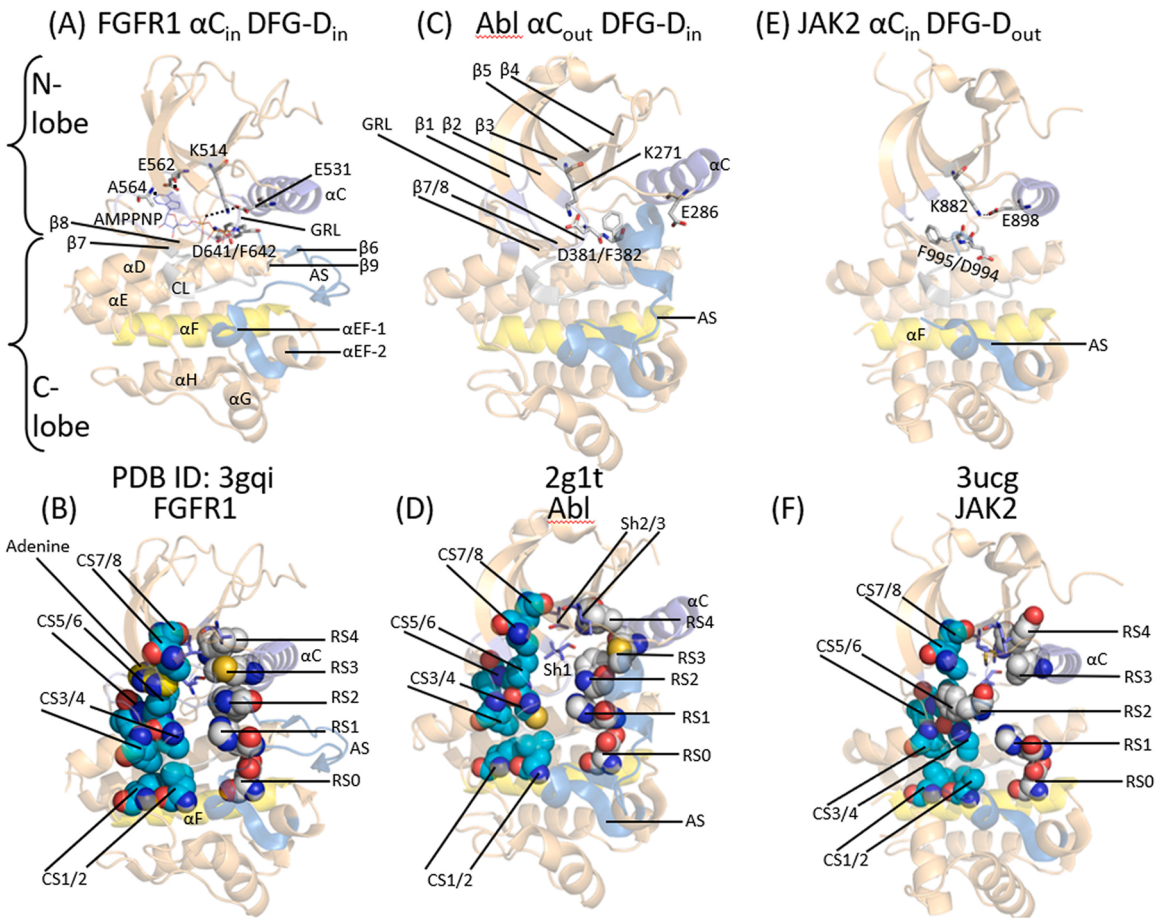

Fig. 1. (A) Overview of active FGFR1 with bound AMP-PNP (adenylyl imidodiphosphate) and (B) its C-spine and R-spine residues. (C) The αC$_{out}$ and DFG-D$_{in}$ structure of dormant Abl and (D) its C-spine, R-spine, and shell residues. (E) Overview of the DGF-D$_{out}$ αC$_{in}$ structure of JAK2 and (F) its C-spine and R-spine residues. AS, activation segment; CL, catalytic loop. GRL, glycine-rich loop. Figs. 1, 2, 5, and 6 were prepared using the PyMOL Molecular Graphics System Version 1.5.0.4 Schrödinger, LLC.

Table 2
Important residues in selected human protein kinases.

	JAK1	JAK2	FGFR1	FGFR2	Abl
Number of residues	1154	1132	822	821	1130
Signal peptide	None	None	1–21	1–21	None
Extracellular segment	None	None	22–376	22–377	None
Transmembrane segment	None	None	377–397	378–398	None
Intracellular portion	1–1154	1–1132	398–822	399–821	1–1130
Protein kinase domain	875–1153	849–1132	478–767	481–770	292–493
Glycine-rich loop	^{882}GEGHFG^{887}	^{856}GKGNFG^{861}	^{485}GEGCFG^{490}	^{488}GEGCFG^{493}	^{249}GGGQYG^{254}
The β3-*K* of *K*/E/D/D	K908	K882	K514	K517	K271
αC-*E* of K/*E*/D/D	E925	E898	E531	E534	E286
Hinge-linker residues	^{957}EFLPSGS^{963}	^{930}YEYLPYGS^{936}	^{562}EYASKGN^{568}	^{565}EYASKGN^{571}	^{316}EFMTYGN^{322}
Gatekeeper residue	M596	M929	V561	V564	T315
Catalytic HR*D* residue, the first *D* of K/E/*D*/D	D1003	D976	D623	D626	D344
Catalytic loop	^{1001}HRDLAARN^{1008}	^{974}HRDLATRN^{981}	^{621}HRDLAARN^{628}	^{624}HRDLAARN^{631}	^{361}HRDLAARN^{368}
AS[a] *D*FG, the second *D* of K/E/D/*D*	D1021	D994	D641	D644	D381
AS[a] tyrosine phosphorylation site	Y1034/5	Y1007/Y1008	Y653/654	Y656/7	Y393
End of the AS[a]	^{1049}APE^{1051}	^{1022}APE^{1024}	^{668}APE^{670}	^{671}APE^{673}	^{407}APE^{409}
Molecular weight (kDa)	133.3	130.7	91.9	92.0	122.8
UniProtKB ID	P23458	O60674	P11362	P21802	P00519–1

[a] AS, activation segment.

expression of maximal enzyme activity in nearly all protein kinases. ErbB1/2/4 of the EGFR family are a notable exception because they exhibit maximal activity in the absence of activation segment phosphorylation. The activation segment DFG occurs spatially near the conserved catalytic loop HRD sequence and the amino-terminus of the αC-helix. The regulatory αC-helix, which occurs within the amino-terminal lobe, nevertheless occupies a strategically important position between both lobes. The protein kinase activation segment has an extended and open structure in the functional form of all protein kinases (Fig. 1A) and a closed structure in most inactive kinases (Fig. 1C/E) [2]. The first two activation segment residues occur in different conformations. The DFG-D side chain of active protein kinases

points toward the ATP-binding site and it binds Mg^{2+}(1). This structure is known as the "DFG-D_{in}" conformation (Fig. 1A/C). The DFG-D side chain in many inactive protein kinases points away from the ATP-binding site. This structure is known as the "DFG-D_{out}" conformation (Fig. 1E). It is the property of DFG-D to bind (DFG-D_{in}) or not bind (DFG-D_{out}) Mg^{2+}(1) within the active site that is important.

Modi and Dunbrack analyzed the interaction of drugs with active and inactive conformations of protein kinases based upon the structure of the activation segment, which begins with the canonical DFG sequence [27,28]. As noted, this sequence is seen in two major conformations: DFG-D_{in} and DFG-D_{out}. In the first instance the phenylalanine residue interacts with the αC-helix of the aminoterminal lobe and in the second instance the phenylalanine is found in a portion of the physiological ATP site thereby generating an αC-helix pocket. These investigators found a constellation of protein kinase conformations that depended on the location of the phenylalanine side chain (DFG-D_{in}, DFG-D_{out}, and DFG-$D_{intermediate}$) and the backbone dihedral angles of the xDF sequence where x is the residue before the DFG signature. They identified eight different conformations and classified them based on the configuration (χ1) of the phenylalanine rotamer (minus, plus, trans) and on the Ramachandran regions (A, alpha; B, beta; L, left) of the xDF motif. Their clusters divide the DFG-D_{in} configuration into six groups including BLAminus, which corresponds to active structures, and two common inactive forms, BLBplus and ABAminus. DFG-D_{out} structures occur principally in the BBAminus conformation. The inactive conformations possess features that inhibit their interaction with Mg^{2+}, ATP, and/or their protein substrates. Modi and Dunbrack produced a searchable and noncommercial web site (http://dunbrack3.fccc.edu/kincore/) that allows one to determine whether a protein kinase conformation corresponds to an active enzyme (DFG-D_{in}, BLAminus) or to an inactive enzyme (DFG-D_{in}, BLBplus, DFG-D_{in}, ABAminus, DFG-D_{out}, BBAminus). We used this web site to determine whether the structure of our various drug-enzyme complexes correspond to active (DFG-D_{in}, BLAminus) or dormant (otherwise) enzymes. Table 3 presents a comparison of the Modi-Dunbrack and our BRIMR schemes. See Refs. [2,27,28] for more material about these and related DFG activation segment arrangements.

2.2. Protein kinase hydrophobic skeletons

Kornev et al. analyzed the three-dimensional structures of active and dormant conformations of about two dozen protein kinases to identify structurally and functionally critical residues [29,30]. Their studies revealed a grouping of four amino acids that make up an R-spine (regulatory spine) and eight amino acids along with the adenine base of ATP that make up a C-spine (catalytic spine). These residues occur in both the N-terminal and C-terminal lobes. These spines generate a stable, but flexible, catalytically active ensemble. The R-spine positions the protein substrate and the C-spine positions ATP for catalysis. The R-spine contains components from both the activation segment and αC-helix, whose structures are important in determining active and inactive enzyme states. The precise positioning and alignment of both spines are necessary, but not sufficient, for the creation of catalytically competent protein kinases.

The R-spine contains the first residue of the β4-strand and the amino acid that is four residues carboxyterminal to the conserved αC-helix glutamate, both of which are within the N-terminal lobe [29]. The R-spine also contains the DFG-phenylalanine of the activation segment and the HRD-histidine of the catalytic loop, both within the C-terminal lobe. The HRD-histidine N–H backbone hydrogen bonds with the side chain of a conserved aspartate within the hydrophobic αF-helix. From the bottom to the top, Meharena et al. labeled the R-spine residues as RS0, RS1, RS2, RS3, and RS4 [31]. We later labeled the C-spine residues from the base to the apex as residues CS1–8 (Fig. 1B/D/F) [32]. Note that the R- and C-spines of active protein kinases are linear (Fig. 1B). RS3 is displaced toward the right in protein kinases with the αC$_{out}$ structure (Fig. 1D). In kinases with the DFG-D_{out} structure, the DFG-D residue (RS2) is displaced toward the left and the R-spine is broken (Fig. 1F). The identity of the C-spine, R-spine, and shell residues of the protein kinases considered in this article are provided in Table 4.

The protein kinase spine and shell residues perform an important role in determining the structure and activity of these enzymes; one cannot overemphasize their importance in supporting the activity of this enzyme superfamily as well as their participation in their interactions with small molecule protein kinase antagonists. For an examination of the properties of the spine and shell residues and their interactions with low molecular weight inhibitors of important members of the protein kinase superfamily, see the following articles: Refs. [33–35] for the ALK pleotrophin and midkine receptor protein-tyrosine kinase, Refs. [16, 36–38] for the EGFR family of protein-tyrosine kinases, Ref. [39] for the PDGFRα/β protein-tyrosine kinases, Ref. [40] for the fibroblast growth factor receptor family of protein-tyrosine kinases, Ref. [41] for the Kit stem cell receptor protein-tyrosine kinase, Ref. [42] for the RET glial-cell derived receptor protein-tyrosine kinase, Ref. [43] for the VEGFR1/2/3 protein-tyrosine kinases, Ref. [44] for the ROS1 orphan receptor protein-tyrosine kinase, Ref. [45] for the Flt3 receptor protein-tyrosine kinase, Refs. [21,46] for the BCR-Abl nonreceptor protein tyrosine kinases, Ref. [47,48] for the Janus nonreceptor protein-tyrosine kinase, Refs. [16,49] for the Bruton nonreceptor protein-tyrosine kinase, Refs. [50,51] for the Src nonreceptor protein-tyrosine kinase, Refs. [52,53] for the MEK1/2 dual specificity protein kinases, Refs. [20,54] for the cyclin-dependent protein-serine/threonine kinase family, Refs. [55,56] for the ERK1/2 protein-serine/threonine kinases, Refs. [57,58] for the RAF protein-serine/threonine kinases, and Ref. [9] for PI 3-kinase, a member of the atypical protein kinase group.

The catalytic spines of protein kinases consist of two residues from the small lobe and six residues from the large lobe. The adenine moiety of ATP unites these two parts of the C-spine and this process enables the functional merging of the two lobes of the enzyme and enables catalysis [30]. The two N-terminal lobe residues that bind to the adenine moiety of ATP include the invariant β2-strand valine (CS7) after the glycine-rich loop and the invariant β3-strand alanine (CS8) of the AxK motif. A hydrophobic amino acid side chain from the middle of the large lobe β7-strand (CS6) interacts with the adenine component of ATP. Additionally, the β-7 strand CS4 and CS5 residues interact with CS3 at the beginning of the αD-helix. Furthermore, CS3 makes hydrophobic contact with (i) the neighboring CS4 and (ii) CS1 within the αF-helix below it. Both the C- and R-spines interact with the hydrophobic αF-helix below them; the αF-helix contains CS1, CS2, and RS0 and it serves as a major foundation for the stabilization of the entire protein kinase domain (Fig. 1). The protein kinase hinge and linker residues connect the N-terminal and C-terminal lobes of protein kinases and the 6-amino N–H group of ATP hydrogen bonds with the backbone carbonyl group of the first hinge residue. Also, the *N*1 of the adenine group of ATP forms a hydrogen bond with the backbone N–H group of the third hinge residue (Fig. 1A). Almost all ATP small-molecule steady-state competitive protein kinase blockers form a hydrogen bond with backbone hinge residues, usually with that of the third hinge residue [32].

Based upon site-directed mutagenesis experiments, Meharena et al. discovered three residues in murine protein kinase A that strengthen and stabilize the regulatory spine, which they identified as shell residues (Sh1, Sh2, and Sh3) [31]. Their Sh1 mutant (V104G) had 5% of the catalytic activity of the normal enzyme and their Sh2/Sh3 double mutant (M120G/M118G) was devoid of all catalytic activity. These findings show that the shell residues support PKA activity. We hypothesize that the corresponding shell residues play a similar stabilizing role for all protein kinases. The Sh1 residue occurs within the segment connecting the αC-helix with the β4-strand, the so-called back loop. The Sh2 residue (the gatekeeper) occurs at the end of the β5-strand immediately before the hinge segment and the Sh3 residue is found two residues upstream from the Sh2 residue within the β5-strand.

The word gatekeeper exemplifies the function that this residue plays in controlling access to the hydrophobic pocket adjoining the adenine

Table 3
Blue Ridge Institute for Medical Research (BRIMR), Modi-Dunbrack Fox Chase Cancer Center (FCCC), and Kinase Ligand Interaction and Fingerprint and Structure (KLIFS) inhibitor data base comparisons.

Ligand/Drug-enzyme	PDB ID	BRIMR type[a]	FCCC type[b,c]	FCCC: Dihedral angles & DFG-D[c]	KLIFS pockets[d]
ADP-AurkA	4dee	I	I	BLAminus & DFG-D_{in}	F, FP-II
BRIMR type I inhibitors					
Bosutinib-Src	4mxo	I	I	BLAminus & DFG-D_{in}	F,G, BP-I-A/B
Dasatinib-Abl	2gqg	I	I, I½b	BLAminus & DFG-D_{in}	F, G, B, BP-I-A/B
Erlotinib-EGFR	1m17	I	I	BLAminus & DFG-D_{in}	F, G, B, BP-I-A/B
Gefitinib-EGFR	2ity	I	I	BLAminus & DFG-Din	F,G, BP-I-A/B
Palbociclib-CDK6	2euf	I	I	BLAminus & DFG-D_{in}	F
Pralsetinib-RET	7ju5	I	I	BLAminus & DFG-D_{in}	F, FP-II
R406 (fostamatinib)	3fqs	I	I	BLAminus & DFG-D_{in}	F
Selpercatinib-RET	7ju6	I	I½f	BLAminus & DFG-D_{in}	F, FP-II
Vandetanib-RET	2ivu	I	I	BLAminus & DFG-D_{in}	F,G, BP-I-A/B
BRIMR type I½A inhibitors					
Dabrafenib-B-Raf	5csw	I½A	I½b	BLBminus & DFG-D_{in}	F, G, B, BP-I-A/B, BP-II-in, BP-II-A-in
Erdafitinib-FGFR1	5ew8	I½A	I½b	BLAplus & DFG-D_{in}	F, G, B, BP-I-A/B
Infigratinib-FGFR1	3tt0	I½A	I½b	BLAplus & DFG-D_{in}	F, G, B, BP-I-A/B
Lapatinib-EGFR	1xkk	I½A	I½b	BLAplus & DFG-D_{in}	F, G, B, BP-I-A/B, BP-II-in, BP-II-A-in
Lenvatinib-VEGFR2	3wzd	I½A	I	BLBplus & DFG-D_{in}	F, G, B, BP-I-B, BP-II-in
Vemurafenic-B-Raf	3og7	I½A	I½b	BLAplus & DFG-D_{in}	F, G, B, FP-I, BP-I-A/B, BP-II-in, BP-II-A-in
BRIMR type I½B inhibitors					
Abemeciclib-CDK6	5l2s	I½B	I	BLBplus & DFG-D_{in}	F, FP-II
Abrocitinib-JAK1	6bbu	I	I	ABAminus & DFG-D_{in}	F, FP-I/II
Abrocitinib-JAK2	6bbv	I	I	ABAminus & DFG-D_{in}	F, FP-I/II
Alectinib-ALK	3aox	I½B	I	ABAminus & DFG-D_{in}	F, BP-I-B
Baricitinib-JAK2	6wto	I½B	I	ABAminus & DFG-D_{in}	F, FP-I/II
Brigatinib-ALK	6mx8	I½B	I	ABAminus & DFG-D_{in}	F, FP-I
Ceritinib-ALK	4mkc	I½B	I	ABAminus & DFG-D_{in}	F, FP-I
Crizotinib-ALK	2xp2	I½B	I	ABAminus & DFG-D_{in}	F, FP-I
Crizotinib-MET	2wgj	I½B	I	BLBplus & DFG-D_{in}	F, FP-I
Crizotinib-ROS1	3zbf	I½B	I	ABAminus & DFG-D_{in}	F, FP-I
Entrectinib-TRKA	5kvt	I½B	I	ABAminus & DFG-D_{in}	F, FP-I
Erlotinib-EGFR	4hjo	I½B	I	BLBtrans & DFG-D_{in}	F, G, BP-I-A/B
Lorlatinib-ALK	4cli	I½B	I	ABAminus & DFG-D_{in}	F, FP-I
Palbociclib-CDK6	5l2i	I½B	I	BLBplus & DFG-D_{in}	F
Ribociclib-CDK6	5l2t	I½B	I	BLBplus & DFG-D_{in}	F, G, FP-I
Ruxolitinib-JAK2	6vgl	I½B	I	ABAminus & DFG-D_{in}	F, FP-I/II
Tepotinib-MET	4r1v	I½B	I	BLBplus & DFG-D_{in}	F, FP-I
Tofacitinib-JAK1	3eyg	I½B	I	ABAminus & DFG-D_{in}	F, FP-I/II
Tofacitinib-JAK3	3lxk	I½B	I	ABAminus & DFG-D_{in}	F, FP-I/II
BRIMR type IIA inhibitors					
Axitinib-VEGFR2	4ag8	IIA	I	BBAminus & DFG-D_{out}	F, G, B, BP-I-B, BP-II-out
Imatinib-Abl[e]	1iep	IIA	II	BBAminus & DFG-D_{out}	F, G, B, BP-I-A/B, BP-II-out, BP-IV
Imatinib-Kit	1t46	IIA	II	BBAminus & DFG-D_{out}	F, G, B, BP-I-A/B, BP-II-out, BP-IV
Imatinib-PDGFRα	6jol	IIA	II	BBAminus & DFG-D_{out}	F, G, B, BP-I-A/B, BP-II-out, BP-IV
Nilotinib-Abl	3cs9	IIA	II	BBAminus & DFG-D_{out}	F, G, B, BP-I-A/B, BP-II-out, BP-V
Pexidartinib-CSF1R	4r7h	IIA	II	BBAminus & DFG-D_{out}	F, G, B, BP-I-B, BP-II-out, BP-V
Ponatinib-Abl[e]	3oxz	IIA	II	BBAminus & DFG-D_{out}	F, G, B, BP-I-A/B, BP-II-out, BP-III, BP-IV
Ponatinib-Kit	4u0i	IIA	II	BBAminus & DFG-D_{out}	F, G, B, BP-I-A/B, BP-II-out, BP-III, BP-IV
Ponatinib-B-Raf	1uwh	IIA	II	BBAminus & DFG-D_{out}	F, G, B, BP-I-B, BP-II-out, BP-III
Ripretinib-Kit	6mob	IIA	II	BBAminus & DFG-D_{out}	F, G, B, BP-I-A/B, BP-II-out, BP-III
Sorafenib-B-Raf	1uwh	IIA	II	BBAminus & DFG-D_{out}	F, G, B, BP-I-B, BP-II-out
Sorafenib-CDK8	3rgf	IIA	II	BBAminus & DFG-D_{out}	F, G, B, BP-I-B, BP-II-out, BP-III
Sorafenib-VEGFR2	4asd	IIA	II	BBAminus & DFG-D_{out}	F, G, B, BP-I-B, BP-II-out, BP-III
Tivozantinib-VEGFR2	4ase	IIA	II	BBAminus & DFG-D_{out}	F, G, B, BP-I-B, BP-II-out
BRIMR type IIB inhibitors					
Bosutinib-Abl	3ue4	IIB	I	Unassigned & DFG-D_{out}	F, G, BP-II-A/B
Gilteritinib-Flt3	6jqr	IIB	I	Unssigned & DFG-D_{out}	F
Nintedanib-VEGFR2	3c7q	IIB	I	Unassigned & DFG-D_{out}	F, G, BP-I-B
Sunitinib-Kit	3g0e	IIB	I	Unassigned & DFG-D_{out}	F
Sunitinib-VEGFR2	4agd	IIB	I	BBAminus & DFG-D_{out}	F, BP-I-B
BRIMR type III inhibitors					
Cobimetinib-MEK1	4an2	III	III, I	BLBplus & DFG-D_{in}	G, B, BP-II-in
Selumetinib-MEK1	4u7z	III	III, I	BLBplus & DFG-D_{in}	G, B, BP-II-in
BRIMR type IV inhibitor					
Asciminib-Abl	5mo4	IV	II, Allosteric	Unassigned & DFG-D_{out}	None
BRIMR type VI inhibitors					
Afatinib-EGFR	4g5j	VI	I	BLAminus & DFG-D_{in}; allosteric	F, G, BP-I-A/B
Dacomitinib-EGFR	4i24	VI	I	BLBtrans & DFG-D_{in}	F, G, BP-I-B
Futibatinib-FGFR1	6mzw	VI	I½b	BLAplus & DFG-D_{in}	F, G, B, BP-I-A/B
Ibrutinib-BTK	5p9j	VI	I½b	BLBplus & DFG-D_{in}	F, G, B, BP-I-B
Neratinib-EGFR	2jiv	VI	I½b	BLBplus & DFG-D_{in}	F, G, B, BP-I-A/B
Osimertinib-EGFR	6jxt	VI	I	BLBtrans & DFG-D_{in}	F
Zanubrutinib-BTK	6j6m	VI	I½b	BLBplus & DFG-D_{in}	F, G, B, BP-I-B

[a] Ref. [32]
[b] b, back; f, front

[c] From Ref. [28] and http://dunbrack3.fccc.edu/kincore/
[d] klifs.net
[e] Mouse enzyme

Table 4
Spine and shell residues of selected human protein kinases.

	Symbol	Klifs No.	JAK1	JAK2	FGFR1	FGFR2	Abl-1a
Regulatory spine							
β4-strand (N-lobe)	RS4	38	Y940	Y913	L547	L550	L301
C-helix (N-lobe)	RS3	28	L929	L902	M535	M538	M290
Activation loop DFG-F (C-lobe)	RS2	82	F1022	F995	F642	F654	F381
Catalytic loop HRD-H (C-lobe)	RS1	68	H1001	H974	H621	H624	H361
F-helix (C-lobe)	RS0	None	D1063	D1036	D682	D685	D421
Shell							
Two residues upstream from the gatekeeper	Sh3	43	L954	L927	V559	V562	I313
Gatekeeper, end of β5-strand	Sh2	45	M956	M929	V561	V564	T315
αC-β4 loop	Sh1	36	V938	V911	I545	I548	V299
Catalytic spine							
β2-strand (N-lobe)	CS8	15	V889	V863	A512	A515	A269
β3-AxK-A (N-lobe)	CS7	11	A906	A880	V492	V495	V256
β7-strand (C-lobe)	CS6	77	L1010	L983	L630	L733	L370
β7-strand (C-lobe)	CS5	78	V1011	V984	V631	V634	V371
β7-strand (C-lobe)	CS4	76	V1009	I982	V629	V632	C369
D-helix (C-lobe)	CS3	53	L964	L937	L569	L572	L323
F-helix (C-lobe)	CS2	None	T1070	V1043	L689	L692	L428
F-helix (C-lobe)	CS1	None	L1074	L1047	I693	I696	I432

[a]From Ref. [21], https://klifs.net/, and https://www.uniprot.org/uniprotkb/.

binding pocket [59,60], a pocket that regularly interacts with numerous small molecule protein kinase blockers. Based upon the results of Meharena et al. [30], only three of the 14 amino acids neighboring RS3 and RS4 in PKA are conserved. It is important to realize that many small molecule therapeutic steady-state ATP-competitive protein kinase inhibitors interact with the R-spine (RS2/3), the C-spine (CS6/7/8), and shell (Sh1 and Sh2) residues. Ung et al. found that approximately three-quarters of protein kinases have a relatively large gatekeeper residue (e.g., Met, Leu, Phe) while about one-quarter have smaller gatekeeper residues (e.g., Thr, Val) [61]. Also of significance in the issue of long-term drug efficacy, the gatekeeper residue of inhibitor target protein kinases is one of the more common sites of drug-resistant mutations [3,62].

3. Classification of protein kinase-inhibitor complexes and description of inhibitor-binding pockets

Based upon earlier studies [60,63–66], we classified the small molecule protein kinase inhibitors into seven main groups including reversible (Groups I, I½, II, III, IV, and V) and targeted covalent irreversible inhibitors (VI) as noted in Table 5. We divided the type I½ and type II antagonists into A and B subtypes [32]. Subtype A drugs continue past the gatekeeper residue into the back cleft. In contrast, subtype B drugs are those that do not extend into the back cleft. The possible importance of this difference, based on incomplete data, is that subtype A blockers bind to their enzyme target with longer residence times when compared with subtype B blockers [32]. For example, sorafenib is a type IIA VEGFR blocker and sunitinib is a type IIB VEGFR inhibitor, both of which are FDA-approved for the treatment of renal cell carcinomas. The type IIA blocker has a residence time exceeding 64 min while the type IIB inhibitor has a residence time of less than 2.9 min [32].

Table 5
Classification of small molecule protein kinase inhibitors[a].

Inhibitor type	Properties
I	Binds in and around the ATP-binding pocket of an active enzyme
I½ A/B	Binds in and around the ATP-binding pocket of an inactive DFG-D_{in} enzyme
I½ A	Extends into the back cleft
I½ B	Does not extend into the back cleft
II A/B	Bind in and around the ATP-binding site of an inactive DFG-D_{out} enzyme
II A	Extends into the back cleft
II B	Does not extend into the back cleft
III	Allosteric inhibitor bound next to the ATP-binding site
IV	Allosteric inhibitor bound away from the ATP-binding site
V	Bivalent inhibitor spanning two kinase domain regions
VI	Covalent inhibitor

[a] Adapted from Ref. [32].

We followed the work of Liao, van Linden et al., Kooistra et al., and Kanev et al. [66–69] in defining and differentiating drug-binding pockets. A synopsis depicting the location of the pockets and subpockets is provided in Fig. 2 and the position of important residues lining these pockets is described in Table 6. The region between the small and large protein kinase lobes is divided into a front cleft or pocket, a gate area, and a back cleft. The back pocket (hydrophobic pocket II, or HPII) includes the gate area and the neighboring back cleft. The front cleft contains the hinge residues, the linker residues that connect the hinge residues to the αD-helix in the large lobe, the glycine-rich loop (GRL), the adenine-binding pocket (AP), and the catalytic loop $(HRD(x)_4N)$.

Type I inhibitors typically bind within the front cleft. The gate area includes residues from both the amino-terminal and carboxyterminal lobes. The gate area contains two residues from the β3-strand and two proximal residues from the β3-αC loop. It also includes the residue immediately before the activation segment (the x of xDFG) together with the first five residues of the activation segment. The back cleft includes the middle of the αC-helix, the β4-strand, and three residues from the β5-strand. The back cleft also contains five residues from the large lobe αE-helix and the three residues before the catalytic loop HRD. Many type I½ inhibitors occupy both the front cleft and a portion of the back cleft. One of the general objectives in the design of small molecule protein kinase inhibitors is to maximize selectivity to minimize off-target side effects [64]; this approach can be aided by comparing drug interactions with target and nontarget kinases [70–72]. Producing drug fragments that bind to residues that line the various pockets plays a strategic role in protein kinase inhibitor discovery with the objective of maximizing drug affinity.

van Linden et al. [67] and Kanev et al. [69] described drug and ligand binding to more than 5200 human and mouse protein kinases.

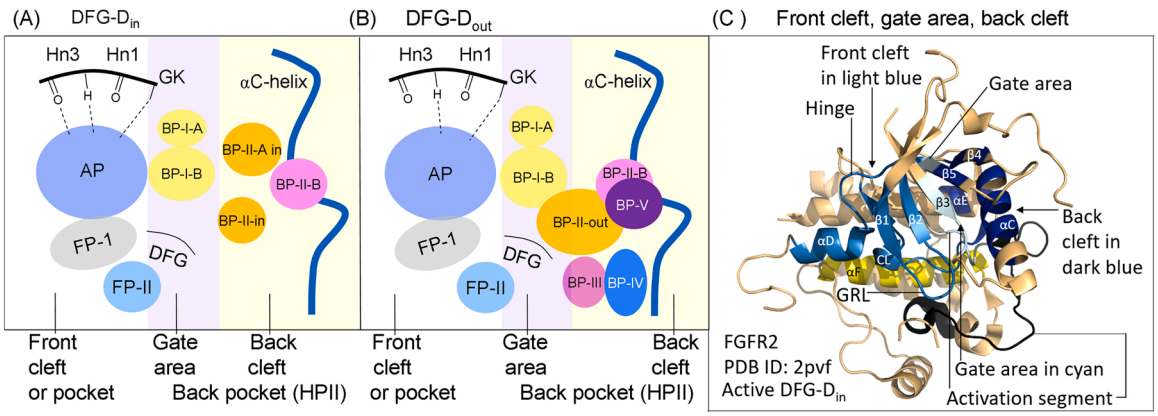

Fig. 2. (A) Location of the protein kinase domain drug-binding pockets in the DFG-D_{in} enzyme form. (B) Location of the drug-binding pockets in the DFG-D_{out} enzyme form. (C) Location of the protein kinase front cleft, gate area, and back cleft. AP, adenine pocket; BP, back pocket; FP, front pocket; Hn, hinge; HPII, hydrophobic pocket II; GK, gatekeeper.
(B) Adapted from Refs. [66–69].

Table 6
Location of important residues within the front cleft, gate area, and back cleft.

Description	Location	KLIFS residue no.[a]
GxGxΦG	Front cleft	4–9
β2-strand V (CS7)	Front cleft	11
β3-strand A (CS8)	Front cleft	15
HRD with DFG-D_{in}	Front cleft	68–70
$HRD(x)_4N$-N	Front cleft	75
β7-strand CS6	Front cleft	77
β3-strand K	Gate area	17
αC-β4 penultimate back loop residue	Gate area	36
Gatekeeper	Gate area	45
The x of xDFG	Gate area	80
DFG	Gate area	81–83
αC-helix E	Back cleft	24
RS3	Back cleft	28
HRD with DFG-D_{out}	Back cleft	68–70

[a] Refs. [67–69].

Their KLIFS (kinase–ligand interaction fingerprint and structure) compendium includes an alignment of 85 ligand binding-site residues that are found in both the small and large lobes; their catalog facilitates the evaluation of drugs and ligands based upon their binding characteristics. Such information helps in the detection of common and unique drug-enzyme interactions. These investigators devised a standard amino acid residue numbering system that facilitates the comparison of different protein kinases and their ligands. Table 6 depicts the relationship of the KLIFS database nomenclature and the C-spine, R-spine, and shell amino acid residue numbering system and Fig. 3 illustrates the location of the KLIFS residues within the protein kinase domain. Providing considerable help to the protein kinase community, these authors produced a valuable searchable and noncommercial web site that is regularly updated that provides comprehensive information on the interaction of protein kinases with drugs and ligands (klifs.net).

Additionally, Carles et al. launched a comprehensive listing of protein kinase inhibitors that are in clinical trials or that have been approved by various regulatory agencies [6]. They produced a searchable and noncommercial web site that is regularly updated that includes the structure and physical properties of the various drugs, their protein kinase targets, their therapeutic indications, the year of first approval by regulatory agencies (if applicable), and their trade names (http://www.icoa.fr/pkidb/). Similarly, the Blue Ridge Institute for Medical Research (BRIMR) maintains a web site that lists the FDA-approved protein kinase blockers and provides their (i) molecular structures, (ii) the number of hydrogen bond donors/acceptors, (iii) the calculated Log of the partition and distribution coefficients, (iv) the number of rings and rotatable

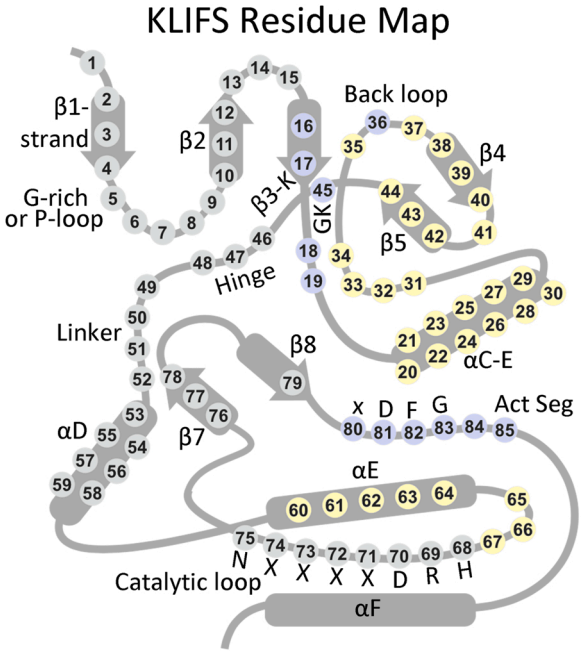

Fig. 3. The location of the KLIFS residues within a generic protein kinase domain. Act Seg, activation segment. Residues in gray circles are found in the front cleft; blue circles, gate area; yellow circles, back cleft.

bonds, (v) the year of initial approval, (vi) their primary protein kinase targets, (vii) and their clinical indications. The website also provides a link to the corresponding FDA labels. This website, which is found at www.brimr.org/PKI/PKIs.htm, is updated following FDA-approval of new protein kinase antagonists.

4. Drug-enzyme interactions: abrocitinib, futibatinib, asciminib

4.1. Abrocitinib-JAK1/2 complexes

Abrocitinib is a pyrrolopyrimidine derivative (Fig. 4A) that is FDA-approved for the management of atopic dermatitis (Table 1). It is a potent JAK1 blocker (IC_{50} = 5.01 nM) with moderate activity against JAK2 (IC_{50} = 39.8 nM) and lesser activity against JAK3 (IC_{50} = 501 nM) or TYK2 (IC_{50} = 1260 nM) [48]. Vazquez et al. determined the X-ray structure of abrocitinib bound to JAK1 and they observed that the pyrrolo N–H hydrogen bonds with the backbone carbonyl oxygen of the

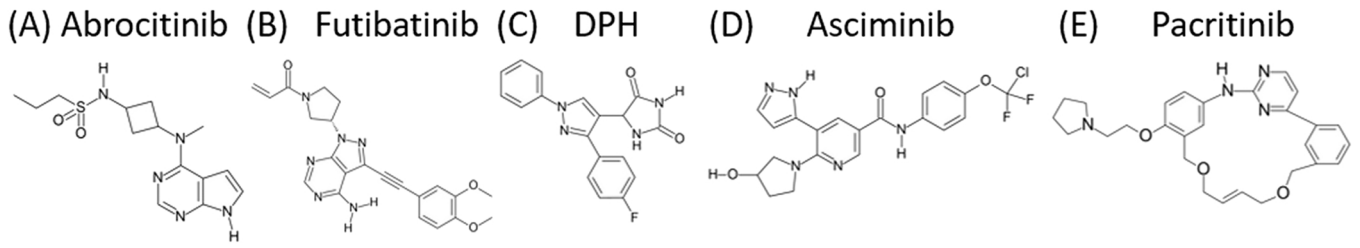

Fig. 4. (A–E). Chemical structures of selected protein kinase ligands.

first hinge residue (E957) and the pyrimidine *N*1 hydrogen bonds with the N–H backbone of the third hinge residue (L959) [73]. Moreover, the amino N–H group of the drug forms hydrogen bonds with the side chain carbonyl group of the catalytic loop asparagine (N1008) and a sulfonamide oxygen of the drug forms a hydrogen bond with the N–H of the side chain of R1007 of the catalytic loop (Fig. 5A). The pyrimidine *N*3 hydrogen bonds with a water molecule that in turn forms a hydrogen bond with E966 within the αD-helix. The corresponding residue in JAK2 is not glutamate but is the shorter aspartate so that this water-mediated hydrogen bond is unable to form. This difference accounts in part for the greater potency of abrocitinib for JAK1 than for JAK2 [73]. The drug makes hydrophobic contact with the first two shell residues (Sh1/2), three catalytic spine residues (CS6/7/8) and KLIFS residues 3, 80, and 81 (Table 7). The KLIFS-3 residue is found immediately before the G-rich loop, KLIFS-80 is the x residue of xDFG, and the KLIFS-81 residue is the DFG-D residue. Abrocitinib also interacts hydrophobically with ^{882}GEG^{884} and G887 within the glycine-rich loop, the β3-strand AxK-K908, and residues F958, L959, G962, and S963 of the hinge-linker segment. Modi and Dunbrack found that this enzyme occurs within the inactive ABAminus enzyme cluster, which they label as a type I inhibitor [28]. The drug occupies the front pocket and FP-I/II and we classify it as a type I½ B inhibitor – inactive DFG-D_{in} with the drug not extending into the back pocket [32]. See Ref. [74,75] for the results of clinical trials that led to the approval of abrocitinib in the United States in 2022; the drug had been approved in the UK and Japan in 2021 [76].

Vazquez et al. determined the X-ray structure of abrocitinib bound to JAK2 and they reported that its interactions mirrored its binding to JAK1 [73]. These authors found that the pyrrolo N–H forms a hydrogen bond with the backbone carbonyl group of the first hinge residue (E930) and the pyrimidine *N*1 forms a hydrogen bond with the N–H backbone of the third hinge residue (L932). Furthermore, a drug sulfonamide oxygen hydrogen bonds with the N–H of the side chain of R980 of the catalytic loop and the N–H of the drug hydrogen bonds with the side chain carbonyl portion of the catalytic loop asparagine (N981) (Fig. 5B). The drug makes hydrophobic contact with the first two shell residues (Sh1/2), three catalytic spine residues (CS6/7/8) and KLIFS residues 3, 80, and 81 (Table 7). The drug also interacts hydrophobically with ^{856}GEG^{858} and G861 of the glycine-rich loop, the β3-strand AxK-K882, and residues Y931, L932, G935, and S936 of the hinge-linker segment. The *N*3 of abrocitinib forms a hydrogen bond with a water molecule in the JAK2-drug complex, but this water molecule is 5.9 Å from the side chain of D939 within the αD-helix – too long to form a hydrogen bond. In contrast, the distance from the comparable water molecule in the JAK1-abrocitinib structure is 3.3 Å from the analogous E966 – which is within hydrogen bonding distance. This difference accounts in part for the greater affinity of abrocitinib for JAK1 than for JAK2 [73]. Modi and Dunbrack found that this enzyme occurs within the inactive ABAminus enzyme cluster, which they label as a type I inhibitor [28]. The drug occupies the front pocket and FP-I/II and we classify it as a type I½ B inhibitor – inactive DFG-D_{in} with the drug not extending into the back pocket [32].

4.2. *Futibatinib*

Futibatinib is a pyrazolo[3,4-*d*]pyrimidine derivative (Fig. 4B) that inhibits FGFR1/2/3/4 with IC_{50} values of 3.9/1.3/1.6/8.3 nM; futibatinib is thereby classified as a pan-FGFR inhibitor [77]. Its inhibitory activity against other protein kinases has not been reported. Futibatinib received FDA approval in 2022 for the treatment of cholangiocarcinomas (bile duct cancers) with FGFR2 fusions or rearrangements (www.brimr.org/PKI/PKIs.htm). We lack the structure of this agent with FGFR2, but Kalyukina et al. determined the X-ray crystal structure of futibatinib covalently bound to the closely related FGFR1 [77]. It shows that the 4-amino group of the pyrimidine forms a hydrogen bond with the carbonyl group of E562 (the first hinge residue) and *N*3 forms a hydrogen bond with the N–H group of A564 (the third hinge residue). The oxygen atom of one of the methoxy groups hydrogen bonds with the backbone N–H group of DFG-D641 while the drug forms a covalent Michael adduct with C488 (Fig. 5C). Futibatinib interacts hydrophobically with five spine residues (RS2/3 and CS6/7/8), all three shell residues (Sh1/2/3), and KLIFS-3 (Table 7). The drug also makes hydrophobic contact with F489 of the glycine-rich loop, the β2-strand V492, the β3-strand AVK-K514, E531 and M535 of the αC-helix, Y563 within the hinge, A640 (the x of xDFG), and DFG-D641. Modi and Dunbrack reported that this enzyme occurs within the inactive BLAplus cluster, which they label as a type I½b blocker. The compound occupies

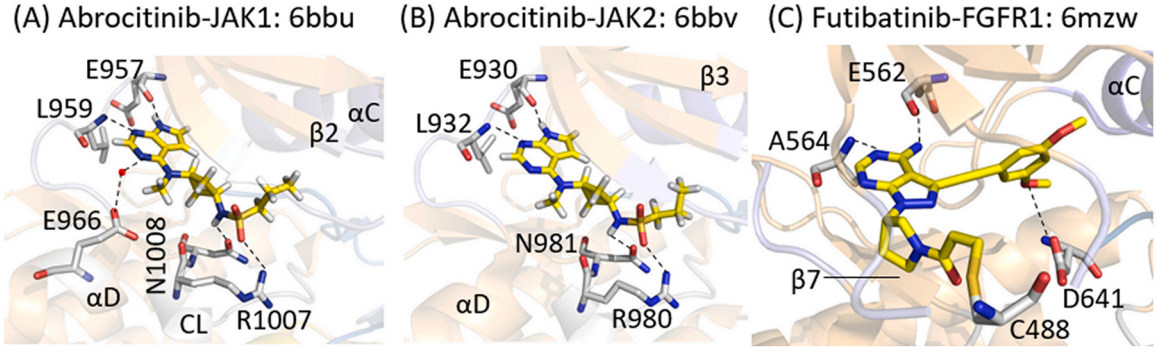

Fig. 5. (A) Abrocitinib-JAK1. (B) Abrocitinib-JAK2. (C) Futibatinib-FGFR1. The respective PDB ID numbers are listed. The drug carbon atoms are colored yellow and the dashed lines represent polar bonds. CL, catalytic loop.

Table 7
Drug-enzyme hydrophobic (Φ) and hydrogen-bond (A, D) interactions based upon their common KLIFS residue numbers[a, b, c, d, e].

	PDB ID	RS1	RS2	RS3	RS4	Sh1	Sh2	Sh3	CS5	CS6	CS7	CS8	KLIFS-3[d]	KLIFS pockets[a]
KLIFS no. →		68	82	28	38	36	45	43	76	77	11	15	3	
Drug-enzyme ↓														
Type I inhibitors														
Bosutinib-Src	4mxo			Φ		Φ	Φ	Φ		Φ	Φ	Φ	Φ	F,G, BP-I-A/B
Dasatinib-Abl	2gqg			Φ		Φ	Φ, A	Φ		Φ	Φ	Φ	Φ	F, G, B, BP-I-A/B
Erlotinib-EGFR	1m17						Φ	Φ		Φ	Φ	Φ	Φ	F, G, B, BP-I-A/B
Gefitinib-EGFR	2ity			Φ			Φ	Φ		Φ	Φ	Φ	Φ	F,G, BP-I-A/B
Palbociclib-CDK6	2euf					Φ	Φ			Φ	Φ	Φ	Φ	F
Pralsetinib-RET	7ju5						Φ			Φ	Φ	Φ	Φ	F, FP-II
R406 (fostamatinib)	3fqs					Φ	Φ			Φ	Φ	Φ	Φ	F
Selpercatinib-RET	7ju6						Φ			Φ	Φ	Φ	Φ	F, FP-II
Vandetanib-RET	2ivu				Φ	Φ	Φ	Φ		Φ	Φ	Φ	Φ	F,G, BP-I-A/B
Type I½A inhibitors														
Dabrafenib–B-Raf	5csw		Φ, D	Φ	Φ	Φ	Φ	Φ		Φ	Φ	Φ	Φ	F, G, B, BP-I-A/B, BP-II-in, BP-II-A-in
Erdafitinib-FGFR1	5ew8		Φ	Φ		Φ	Φ	Φ		Φ	Φ	Φ	Φ	F, G, B, BP-I-A/B
Infigratinib-FGFR1	3tt0			Φ		Φ	Φ	Φ		Φ	Φ	Φ	Φ	F, G, B, BP-I-A/B
Lapatinib-EGFR	1xkk		Φ	Φ	Φ	Φ	Φ	Φ		Φ	Φ	Φ	Φ	F, G, B, BP-I-A/B, BP-II-in, BP-II-A-in
Lenvatinib-VEGFR	3wzd		Φ	Φ		Φ	Φ			Φ	Φ	Φ	Φ	F, G, B, BP-I-B, BP-II-in
Vemurafenib-B-Raf	3og7		Φ	Φ	Φ	Φ	Φ	Φ		Φ	Φ	Φ	Φ	F, G, B, FP-I, BP-I-A/B, BP-II-in, BP-II-A-in
Type I½B inhibitors														
Abemeciclib-CDK6	5l2s					Φ	Φ			Φ	Φ	Φ	Φ	F, FP-II
Abrocitinib-JAK1	6bbu					Φ	Φ			Φ	Φ	Φ	Φ	F, FP-I/II
Abrocitinib-JAK2	6bbv					Φ	Φ			Φ	Φ	Φ	Φ	F, FP-I/II
Alectinib-ALK	3aox					Φ	Φ			Φ	Φ	Φ	Φ	F, BP-I-B
Baricitinib-JAK2	6wto					Φ	Φ			Φ	Φ	Φ	Φ	F, FP-I/II
Brigatinib-ALK	6mx8			Φ			Φ			Φ	Φ	Φ	Φ	F, FP-I
Ceritinib-ALK	4mkc			Φ		Φ				Φ	Φ	Φ	Φ	F, FP-I
Crizotinib-ALK	2xp2			Φ			Φ			Φ	Φ	Φ	Φ	F, FP-I
Crizotinib-MET	2wgj			Φ		Φ	Φ			Φ	Φ	Φ	Φ	F, FP-I
Crizotinib-ROS1	3zbf					Φ	Φ			Φ	Φ	Φ	Φ	F, FP-I
Entrectinib-TRKA	5kvt					Φ	Φ		Φ	Φ	Φ	Φ	Φ	F, FP-I
Erlotinib-EGFR	4hjo			Φ		Φ	Φ			Φ	Φ	Φ	Φ	F, G, BP-I-A/B
Lorlatinib-ALK	4cli									Φ	Φ	Φ	Φ	F, FP-I
Palbociclib-CDK6	5l2i					Φ	Φ			Φ	Φ	Φ	Φ	F
Ribociclib-CDK6	5l2t					Φ	Φ			Φ	Φ	Φ	Φ	F, G, FP-I
Ruxolitinib-JAK2	6vgl					Φ	Φ			Φ	Φ	Φ	Φ	F, FP-I/II
Tepotinib-MET	4r1v					Φ	Φ			Φ	Φ	Φ	Φ	F, FP-I
Tofacitinib-JAK1	6bbu					Φ	Φ			Φ	Φ	Φ	Φ	F, FP-I/II
Tofacitinib-JAK3	3lxk					Φ	Φ		Φ	Φ	Φ	Φ	Φ	F, FP-I/II
Type IIA inhibitors														
Axitinib-VEGFR2	4ag8		Φ	Φ		Φ	Φ	Φ		Φ	Φ	Φ	Φ	F, G, B, BP-I-B, BP-II-out
Imatinib-Abl[f]	1iep	Φ, A	Φ	Φ		Φ	Φ, A	Φ		Φ	Φ	Φ	Φ	F, G, B, BP-I-A/B, BP-II-out, BP-IV
Imatinib-Kit	1t46	Φ	Φ	Φ		Φ	Φ, A	Φ		Φ	Φ	Φ	Φ	F, G, B, BP-I-A/B, BP-II-out, BP-IV
Imatinib-PDGFRα	6jol	Φ, D	Φ	Φ		Φ	Φ, D	Φ		Φ	Φ	Φ	Φ	F, G, B, BP-I-A/B, BP-II-out, BP-IV
Nilotinib-Abl	3cs9	Φ	Φ	Φ		Φ	Φ, A	Φ		Φ	Φ	Φ	Φ	F, G, B, BP-I-A/B, BP-II-out, BP-V
Pexidartinib-CSF1R	4r7h		Φ	Φ		Φ	Φ			Φ	Φ	Φ	Φ	F, G, B, BP-I-B, BP-II-out, BP-V
Ponatinib-Abl[f]	3oxz	Φ, A	Φ	Φ		Φ	Φ	Φ		Φ	Φ	Φ	Φ	F, G, B, BP-I-A/B, BP-II-out, BP-III, BP-IV
Ponatinib-Kit	4u0i	Φ, A	Φ	Φ		Φ	Φ	Φ		Φ	Φ	Φ	Φ	F, G, B, BP-II-A/B, BP-II-out, BP-III, BP-IV
Ponatinib-B-Raf	1uwh	Φ	Φ	Φ		Φ	Φ			Φ	Φ	Φ	Φ	F, G, B, BP-I-B, BP-II-out, BP-III
Ripretinib-Kit	6mob	Φ	Φ	Φ		Φ	Φ	Φ		Φ	Φ	Φ	Φ	F, G, B, BP-I-A/B, BP-II-out, BP-III
Sorafenib-B-Raf	1uwh	Φ	Φ	Φ		Φ	Φ			Φ	Φ	Φ		F, G, B, BP-I-B
Sorafenib-CDK8	3rgf	Φ	Φ	Φ		Φ	Φ			Φ	Φ	Φ	Φ	F, G, B, BP-I-B, BP-II-out, BP-III
Sorafenib-VEGFR2	4asd	Φ	Φ	Φ		Φ	Φ			Φ	Φ	Φ	Φ	F, G, B, BP-I-B, BP-II-out, BP-III
Tivozanib-VEGFR2	4ase		Φ	Φ		Φ	Φ	Φ		Φ	Φ	Φ	Φ	F, G, B, BP-I-B
Type IIB inhibitors														
Bosutinib-Abl	3ue4		Φ	Φ		Φ	Φ	Φ		Φ	Φ	Φ	Φ	F, G, BP-II-A/B
Gilteritinib-Flt3	6jqr		Φ							Φ	Φ	Φ	Φ	F
Nintedanib-VEGFR2	3c7q			Φ		Φ	Φ			Φ	Φ	Φ	Φ	F, G, BP-I-B
Sunitinib-Kit	3g0e		Φ			Φ				Φ	Φ	Φ	Φ	F
Sunitinib-VEGFR2	4agd		Φ			Φ	Φ			Φ	Φ	Φ	Φ	F, BP-I-B
Type III inhibitors														
Cobimetinib-MEK1	4an2		Φ			Φ	Φ	Φ						G, B, BP-II-in
Selumetinib-MEK1	4u7z		Φ			Φ	Φ	Φ						G, B, BP-II-in
Type IV inhibitor														
Asciminib-Abl	5mo4													None
Type VI inhibitors														
Afatinib-EGFR	4g5j			Φ			Φ	Φ		Φ	Φ	Φ	Φ	F, G, BP-I-A/B
Dacomitinib-EGFR	4i24						Φ	Φ		Φ	Φ	Φ	Φ	F, G, BP-I-B
Futibatinib-FGFR1	6mzw		Φ	Φ		Φ	Φ	Φ		Φ	Φ	Φ	Φ	F, G, B, BP-I-A/B
Ibrutinib-BTK	5p9j		Φ	Φ		Φ	Φ	Φ		Φ	Φ	Φ	Φ	F, G, B, BP-I-B
Neratinib-EGFR	2jiv		Φ	Φ	Φ	Φ	Φ	Φ		Φ	Φ	Φ	Φ	F, G, B, BP-I-A/B
Osimertinib-EGFR	6jxt									Φ	Φ	Φ	Φ	F
Zanubrutinib-BTK	6j6m		Φ	Φ		Φ	Φ	Φ		Φ	Φ	Φ	Φ	F, G, B, BP-I-B

[a] klifs.net.
[b] Human enzyme unless otherwise noted.

[c] Drugs not previously reviewed (Refs [10–13]) are indicated in **bold** print.
[d] KLIFS-3, kinase-ligand interaction fingerprint and structure residue-3.
[e] A, hydrogen-bond acceptor; D, hydrogen-bond donor.
[f] Mouse enzyme

the front cleft, gate area, back cleft and BP-I-A and BP-I-B. Owing to the covalent nature of this interaction, we classify the drug as a type VI (covalent) inhibitor [32]. See Refs. [78–80] for a summary of the clinical trials that led to the approval of futibatinib.

4.3. Abl-ligand interactions: myristate, DPH, and asciminib

Alternative splicing of Abl-1 pre-mRNA yields two transcripts: 1a and 1b. The latter protein is 19 residues longer than Abl-1a and it bears a covalently attached myristoyl group that is added post-translationally to a glycine residue immediately following the initiating amino-terminal methionine [81]. The myristoyl group plays a fundamental role in the regulation of Abl-1b activity while the regulation of Abl-1a remains a mystery. The N-terminus of Abl-1b consists of about 60 residues called the cap (not shown), which is followed by the SH3 domain. SH3 domains (≈ 60 amino acid residues) bind to sequences that can adopt a left-handed helical conformation [82]. The SH3 domain is a β-barrel consisting of five antiparallel β-strands and a prominent structure called the RT loop (Fig. 6A). This loop is found at the ends of a surface composed of aromatic and other hydrophobic residues that comprise the recognition site for protein sequences that bear the PxxP motif. The side chain N–H group of N97 of the RT loop of Abl-1b hydrogen bonds with the carbonyl side chain of N250 of the SH2-kinase linker (not shown). The –OH group of S94 of the RT loop forms a hydrogen bond with the carbonyl group of K281 within the β2-β3 loop of the small lobe of the kinase domain (SH1).

The SH3-SH2 connector is a six-residue section that links these two domains. SH2 domains (≈ 100 amino acid residues) bind to distinct amino acid sequences carboxyterminal to phosphotyrosine residues [83]. The Abl-1a/b SH2 domain contains a central three-stranded β-sheet with an α1- and α2-helix at each side (Fig. 6A). The SH2 domain contains two recognition pockets: one binds phosphotyrosine and the other co-ordinates with one or more hydrophobic residues carboxyterminal to the phosphotyrosine. The phosphotyrosine pocket contains a conserved arginine residue (Arg152 in human Abl-1a) that interacts with the negatively charged phosphate. Songyang and Cantley examined the interaction of a library of phosphopeptides to SH2 domains to define preferred docking sequences [84]. The Abl-1a/b SH2 domain selects pYENP in preference to other sequences. The Abl-1a/b SH2 domain, however, binds to a variety of signature residues that differ from this optimal sequence.

The SH3 and SH2 domains interact with the protein kinase (SH1) domain of Abl-1b. The N-terminal and C-terminal lobes of catalytically competent Abl-1b must be able to move (breath) in order to mediate the phosphorylation of its substrates. To keep the Abl-1b kinase in an inactive state, the SH3 domain, the SH2 domain, and the SH2-kinase linker dock tightly to the protein kinase domain and restrict its mobility and inhibit its catalytic activity.

Experiments at the turn of this century helped to elucidate the role of the amino-terminal Abl-1b myristoyl group in the regulation of protein kinase activity [85]. Hantschel et al. discovered that the ABL1b glycine-to-alanine mutation at position 2 (*G2A*) led to the biosynthesis of an enzyme with dramatically higher catalytic activity than wildtype Abl-1b [86]. Conversion of glycine to any other residue prevents the myristoylation as catalyzed by N-myristoyltransferase. The first four residues of Abl-1b are MGQQ, which will promote N-myristoyltranferase activity, and those of Abl-1a are MLEI, which will not. Moreover, unlike the wildtype enzyme, the *G2A* mutant protein was highly phosphorylated. These findings indicated that the myristoyl group acts to negatively regulate Abl-1b phosphotransferase activity.

In a joint study with Hantschel et al. [86], Nagar et al. described the X-ray crystal structure of mouse Abl-1b with myristate [87]. They found that the myristoyl group was lodged in a deep hydrophobic pocket at the bottom of the protein kinase domain containing residues from the αE-helix (A356, L359, L360), the αF-helix (L448, A452, Y454), the αH-helix (C483, P484, V487), and an induced αI'-helix (I521, V525,

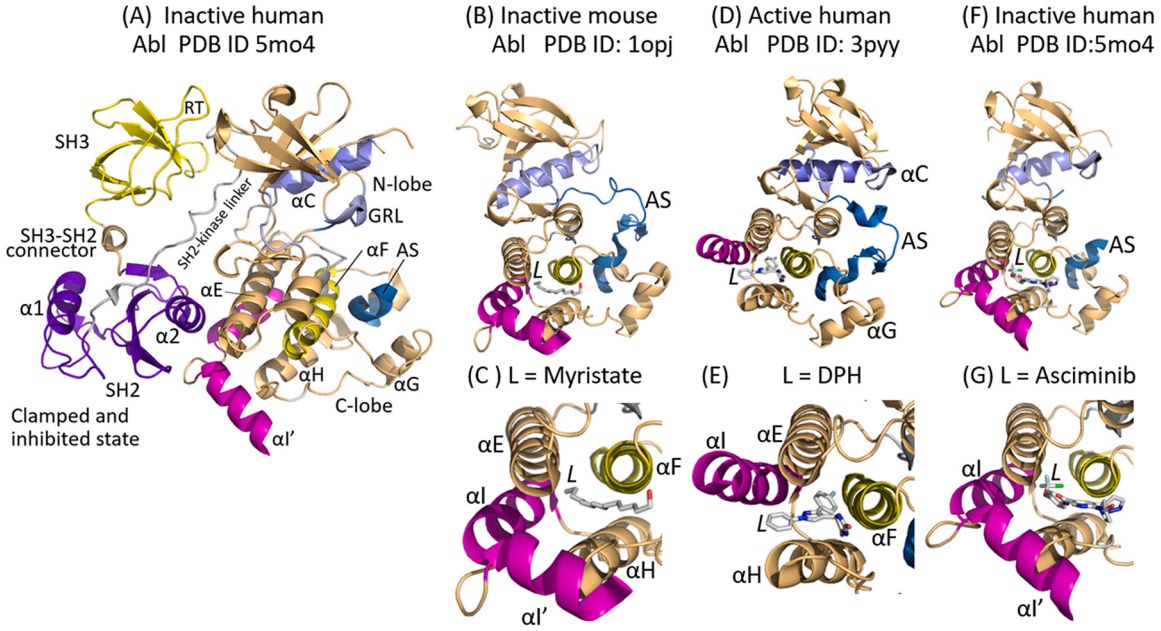

Fig. 6. (A) Overview of the structure of human Abl-1b illustrating the SH3-SH2 inhibitory domains including the RT loop interacting with the protein kinase domain (SH1). (B, C) Myristate bound to mouse Abl. (D, E) DPH bound to human Abl. (F, G) Asciminib bound to human Abl. AS, activation segment; GRL, glycine-rich loop; L, ligand.

L529). The nine terminal carbon atoms of myristate are found within the hydrophobic cavity and carbon atoms C2-C5 occur in an open notch where the side chains of V525 and L529 from the αI'-helix form a ledge for the myristoyl group (Fig. 6B/C). The interaction of myristate with its binding compartment induces a bend in the αI-helix to form αI'. As a result, the SH3-SH2 complex can dock tightly with the SH1 kinase domain thereby blocking its mobility and catalytic activity. Without the αI-helix–induced bend (Fig. 6D/E), the backside of Abl-1b is unable to dock firmly to the protein kinase domain and the enzyme is active. The myristate binding pocket is a type IV allosteric-inhibitor–binding site [88].

Yang et al. used high-throughput screening experiments and identified a small molecule cell permeable activator of Abl (5-(1,3-Diaryl-1 H-Pyrazol-4-yl) Hydantoin)), which they named DPH (Fig. 4 C) [89]. The X-ray crystal structure revealed that it bound to the myristate-binding site of its target. DPH interacts hydrophobically with residues of the αE-helix (A356, L359/360, A363), the αF-helix (L448, I451, A452), and the αH-helix (C483, P484 and V487) (Fig. 6D/E). An N–H group from the hydantoin component forms a hydrogen bond with the carbonyl group of E481 (not shown). It fails to contact the αI-helix and thus it cannot induce a bend in the αI-helix thereby explaining its activating effect.

Using NMR methodology, Schoepfer et al. examined about 500 soluble ligand fragments that bound to Abl-1 [90]. X-ray crystallography showed that their compounds bound to the Abl myristate-binding site and they subsequently used standard medicinal chemistry approaches to increase drug solubility. These experiments were followed by work on lead-compounds that inhibited tumor growth in (i) cell culture and in (ii) murine subcutaneous xenograft models of CML. After the development of asciminib (Fig. 4D), they performed a comprehensive examination of drug properties and found that it targeted Abl and had little activity against a constellation of other protein kinases. The X-ray crystal structure of asciminib with Abl-1b shows that it makes hydrophobic contact with R351, A356, L359/360, A363 of the αE-helix, L448 and ^{451}IATY^{454} of the αF helix, C483, P484, V487 of the αH-helix, F512 of the αI-helix, and I521, V525, and L529 of the αI'-helix. The drug also forms a hydrogen bond with E481 (not shown). Of importance, asciminib is active against the *T315I* (Abl-1a nomenclature) gatekeeper mutant. The drug binds to an allosteric site that is far from the ATP-binding site (28 Å) and is now the best example of an FDA-approved type IV antagonist. Asciminib is FDA-approved for the third line treatment of Philadelphia chromosome-positive CML and the first line treatment of Philadelphia chromosome-positive CML with the *T315I* mutation. See Ref. [91] for a summary of the clinical trials that led to the FDA approval of this STAMP (specifically targeting the Abl myristoyl pocket) inhibitor.

5. Pacritinib, an approved protein kinase antagonist lacking a drug-kinase structure

Pacritinib is an anilino-pyrimidine derivative (Fig. 4E) that is FDA-approved for the treatment of myelofibrosis [92]. Myelofibrosis is a myeloid malignancy associated with a heavy symptomatic burden that decreases the quality of life and presents a risk for leukemic transformation. The discovery that the dysfunction of the Janus kinase/signal transducer and activator of transcription (JAK/STAT) pathway plays a role in the pathogenesis of this disorder has led to many clinical investigations for new treatments. Pacritinib is a novel selective inhibitor of JAK2 and FMS-related tyrosine kinase 3 (Flt3). It received its first approval in February 2022 in the United States for the treatment of adults with intermediate- or high-risk primary or secondary (post--polycythemia vera or post-essential thrombocythemia) myelofibrosis with a platelet count below 50×10^9/L. The accelerated approval was based on results from the randomized phase III PERSIST-2 trial in which spleen volume reduction was demonstrated in pacritinib recipients. Although we have the X-ray crystal structure of pacritinib bound to the unrelated human quinone reductase 2 (PDB ID: 5LBZ), unfortunately, we lack the X-ray crystal structure of pacritinib with JAK2. For a summary of the clinical trials that led to the approval of this drug, see Refs. [75,92,93].

6. Physicochemical properties of orally effective drugs

6.1. Lipinski's rule of five (Ro5)

Medicinal chemists and pharmacologists have explored the physicochemical properties of drugs that are orally bioavailable. Lipinski's rule of five (Ro5) is an experimental and computational methodology that is used to characterize membrane permeability, solubility, and effectiveness in the drug-discovery setting [94]. It is a rule of thumb that assesses drug-likeness and determines whether a compound with specific pharmacological activities has characteristics suggesting that it would be orally effective. The Lipinski benchmarks were based on data showing that most orally effective medicinals are relatively small and moderately lipophilic substances. The Ro5 criteria are used during drug discovery and development as physiologically active lead compounds are systematically optimized to enhance their activity while maintaining selectivity.

The Ro5 criteria indicates that less than ideal oral bioavailability is more likely to occur when (i) the atom-based calculated Log P (ALogP) is greater than 5, when (ii) there are more than 5 hydrogen-bond donors, when (iii) there are more than 5×2 or 10 hydrogen-bond acceptors, and when (iv) the molecular weight is more than 5×100 or 500 [94]. The partition coefficient (P) is the ratio of the solubility of the un-ionized drug in the organic phase divided by its solubility in the aqueous phase of water-saturated *n*-octanol. The P value mirrors the hydrophobicity of a drug; the greater the P value, the greater the hydrophobicity. The number of hydrogen-bond donors is the sum of NH and OH groups. The number of hydrogen-bond acceptors is more complicated to assess; these are the number of neutral heteroatoms except for halogen atoms, heteroaromatic oxygen and sulfur atoms, pyrrole nitrogen atoms, and higher oxidation states of nitrogen, phosphorus, and sulfur, but it includes the oxygen atoms bonded to them. The Ro5 criteria were based on the physicochemical properties of more than two thousand reference drugs [94].

Excluding the macrolides (everolimus, sirolimus, and temsirolimus), the average molecular weight (MW) of the orally effective FDA-approved protein kinase inhibitors is 478 ranging from 306 (ruxolitinib) to 615 (trametinib) (Table 8). The compounds with a molecular weight greater than 500 include the three macrolides and 24 other drugs. Although this data suggests that there is a propensity for orally bioavailable small molecule protein kinase blockers to exceed the 500 Da molecular-weight criterion, the masses of the larger compounds excepting the macrolides are near 500 Da. Moreover, 18 of the 72 approved drugs have an ALogP of greater than five; these exceptions do not include abrocitinib, asciminib, futibatinib, or pacritinib – the newly approved agents described in this article. Additionally, Tepotinib and trilaciclib have more than five hydrogen bond donors and dabrafenib and fostamatinib have more than ten hydrogen bond acceptors. Overall, a total of 36 of the 72 FDA-approved small molecule protein kinase inhibitors fail to conform to Lipinski's Ro5. Of these 36, bosutinib, brigatinib, cabozantinib, entrectinib, fostamatinib, infigratinib, lapatinib, midostaurin, mobocertinib, neratinib, nilotinib, ripretinib have two Ro5 deficiencies with a molecular weight greater than 500 and a partition coefficient greater than 5. Dabrafenib has three Ro5 deficiencies with a molecular weight greater than 500, an ALogP greater than five, and 11 hydrogen bond acceptors. These are FDA-approved medicines, but finding drug candidates during the discovery process with two or three Ro5 criteria exceptions is typically an undesirable finding.

Table 8
Properties of FDA-approved small molecule inhibitors[a].

Drug	PubMED CID	Formula	MW (Da)	HD[b]	HA[c]	ALogP[d]	Rotatable bonds	PSA[e] (Å^2)	Ring Count[g]	Complexity[f]
Abemaciclib	46220502	$C_{27}H_{32}F_2N_8$	507	1	9	4.94	7	75	5	723
Abrocitinib	78323835	$C_{14}H_{21}N_5S$	323	2	6	1.3	6	99.4	3	474
Acalabrutinib	71226662	$C_{26}H_{23}N_7O_2$	466	2	6	3.31	4	119	5	845
Afatinib	10184653	$C_{24}H_{25}ClFN_5O_3$	486	2	8	4.39	8	88.6	4	702
Alectinib	49806720	$C_{30}H_{34}N_4O_2$	483	1	5	4.77	3	72.4	6	867
Asciminib	72165228	$C_{20}H_{18}ClF_2N_5O_3$	450	4	6	3.46	6	103	4	626
Avapritinib	118023034	$C_{26}H_{27}FN_{10}$	499	1	9	2.61	5	106	6	752
Axitinib	6450551	$C_{22}H_{18}N_4OS$	386	2	4	4.64	5	96	4	557
Baricitinib	44205240	$C_{16}H_{17}N_7O_2S$	371	1	7	1.10	5	129	4	678
Belumosudil	11950170	$C_{26}H_{24}N_6O_2$	452	3	6	4.82	7	105	5	678
Binimetinib	10288191	$C_{17}H_{15}BrF_2N_4O_3$	441	3	7	3.01	6	88.4	3	521
Bosutinib	5328940	$C_{26}H_{29}Cl_2N_5O_3$	530	1	8	5.19	9	82.9	4	734
Brigatinib	68165256	$C_{29}H_{39}ClN_7O_2P$	584	2	9	5.09	8	85.9	5	835
Cabozantinib	25102847	$C_{28}H_{24}FN_3O_5$	501	2	7	5.54	8	98.8	4	795
Capmatinib	25145656	$C_{23}H_{17}FN_6O$	412	1	6	3.43	5	81.5	5	637
Ceritinib	57379345	$C_{28}H_{36}ClN_5O_3S$	558	3	8	6.36	9	114	4	835
Cobimetinib	16222096	$C_{21}H_{21}F_3IN_3O_2$	531	3	7	3.78	4	64.6	4	624
Crizotinib	11626560	$C_{21}H_{22}Cl_2FN_5O$	450	2	6	5.04	5	78	4	558
Dabrafenib	44462760	$C_{23}H_{20}F_3N_5O_2S_2$	520	2	11	5.36	6	148	4	817
Dacomitinib	11511120	$C_{24}H_{25}ClFN_5O_2$	470	2	7	5.16	7	79.4	4	665
Dasatinib	3062316	$C_{22}H_{26}ClN_7O_2S$	488	3	9	3.31	7	135	4	642
Encorafenib	50922675	$C_{22}H_{27}ClFN_7O_4S$	540	3	10	3.91	10	149	3	836
Entrectinib	25141092	$C_{31}H_{34}F_2N_6O_2$	561	3	8	5.03	7	85.5	6	847
Erdafitinib	67462786	$C_{25}H_{30}N_6O_2$	446	1	7	4.18	9	77.3	4	583
Erlotinib	176870	$C_{22}H_{23}N_3O_4$	393	1	7	3.41	11	74.7	3	525
Everolimus	6442177	$C_{53}H_{83}NO_{14}$	958	3	14	6.20	9	205	3	1810
Fedratinib	16722836	$C_{27}H_{36}N_6O_3S$	525	3	9	4.82	11	117	4	787
Fostamatinib	11671467	$C_{23}H_{26}FN_6O_9P$	580	4	15	3.09	10	187	4	904
Futibatinib	71621331	$C_{22}H_{22}N_6O_3$	418	1	7	1.78	6	108	4	723
Gefitinib	123631	$C_{22}H_{24}ClFN_4O_3$	447	1	8	4.28	8	68.7	4	545
Gilteritinib	49803313	$C_{29}H_{44}N_8O_3$	552	3	10	2.70	9	121	5	785
Ibrutinib	24821094	$C_{25}H_{24}N_6O_2$	441	1	6	4.22	5	99.2	5	678
Imatinib	5291	$C_{29}H_{31}N_7O$	494	2	7	4.59	7	86.3	5	706
Infigratinib	53235510	$C_{26}H_{31}Cl_2N_7O_3$	560	2	8	5.35	8	95.1	4	724
Lapatinib	208908	$C_{29}H_{26}ClN_4O_4S$	580	2	9	6.14	11	115	5	898
Larotrectinib	46188928	$C_{21}H_{22}F_2N_6O_2$	428	2	7	2.95	3	86	5	659
Lenvatinib	9823820	$C_{21}H_{19}ClN_4O_4$	427	3	5	4.07	6	116	4	634
Lorlatinib	71731823	$C_{21}H_{19}FN_6O_2$	406	1	7	2.80	0	110	3	700
Midostaurin	9829523	$C_{35}H_{30}N_4O_7$	571	1	4	5.91	3	77.7	5	1140
Mobocertinib	118607832	$C_{32}H_{39}N_7O_4$	586	2	9	5.08	13	114	4	881
Neratinib	9915743	$C_{30}H_{29}ClN_6O_3$	557	2	8	5.93	11	112	4	881
Netarsudil	66599893	$C_{28}H_{27}N_3O_3$	454	2	5	4.89	8	94.3	4	678
Nilotinib	644241	$C_{28}H_{22}F_3N_7O$	530	2	9	6.36	6	97.6	5	817
Nintedanib	135423438	$C_{31}H_{33}N_5O_4$	540	2	7	3.62	8	102	5	947
Osimertinib	71496458	$C_{28}H_{33}N_7O_2$	500	2	7	4.51	10	87.6	4	752
Pacritinib	46216796	$C_{28}H_{32}N_4O_3$	473	1	7	4.96	4	68.7	4	644
Palbociclib	5330286	$C_{24}H_{29}N_7O_2$	448	2	8	2.97	5	103	5	775
Pazopanib	10113978	$C_{21}H_{23}N_7O_2S$	438	2	8	3.14	5	127	4	717
Pemigatinib	86705659	$C_{24}H_{27}F_2N_5O_4$	487	2	7	3.66	6	88.4	5	731
Pexidartinib	25151352	$C_{20}H_{15}ClF_3N_5$	417	2	7	5.23	5	66.5	4	537
Ponatinib	24826799	$C_{29}H_{27}F_3N_6O$	533	1	8	4.46	6	65.8	5	910
Pralsetinib	129073603	$C_{27}H_{32}FN_9O_2$	534	3	9	4.20	8	136	5	816
Regorafenib	11167602	$C_{21}H_{15}ClF_4N_4O_3$	483	3	8	5.69	5	92.4	3	686
Ribociclib	44631912	$C_{23}H_{30}N_8O$	435	2	7	2.80	5	91.2	5	636
Ripretinib	71584930	$C_{24}H_{21}BrFN_5O_2$	510	3	5	5.67	5	86.4	4	746
Ruxolitinib	25126798	$C_{17}N_{18}N_6$	306	1	4	3.47	4	83.2	4	453
Selpercatinib	134436906	$C_{29}H_{31}N_7O_3$	526	1	9	3.28	8	112	6	637
Selumetinib	10127622	$C_{17}H_{15}BrClF_4O_3$	458	3	6	3.53	6	88.4	3	523
Sirolimus	5284616	$C_{51}H_{79}NO_{13}$	914	3	13	6.18	6	195	3	1760
Sorafenib	216239	$C_{21}H_{16}ClF_3N_4O_3$	465	3	7	5.55	5	92.4	3	646
Sunitinib	5329102	$C_{22}H_{27}FN_4O_2$	398	3	4	3.33	7	77.2	3	636
Temsirolimus	6918289	$C_{56}H_{87}NO_{16}$	1029	4	16	4.39	11	242	3	2010
Tepotinib	25171648	$C_{29}H_{28}N_6O_2$	493	7	7	4.01	7	94.7	5	880
Tivozanib	9911830	$C_{22}H_{19}CLIN_4O_5$	455	2	6	5.64	6	108	4	631
Tofacitinib	9926791	$C_{16}H_{20}N_6O$	312	1	5	1.54	3	88.9	3	488
Trametinib	11707110	$C_{26}H_{23}FlN_5O_4$	615	2	6	3.94	5	102	4	1090
Trilaciclib	68029832	$C_{24}H_{30}N_8O$	447	2	7	2.72	3	91.2	6	707
Tucatinib	51039094	$C_{26}H_{24}N_8O_2$	481	2	8	5.09	6	111	6	796
Upadacitinib	58557659	$C_{17}H_{19}F_3N_6O$	380	2	6	2.91	3	78.3	4	561
Vandetanib	3081361	$C_{22}H_{24}BrFN_4O_2$	475	1	7	5.00	6	59.5	4	539
Vemurafenib	42611257	$C_{23}H_{18}ClF_2N_3O_3S$	490	2	7	5.54	7	100	4	790
Zanubrutinib	135565884	$C_{27}H_{27}N_5O_3$	472	2	5	4.22	6	103	5	756

[a] Drugs previously not reviewed (Refs. [10–13]) are given in **bold** type.

[b] No. of hydrogen bond donors.
[c] No. of hydrogen bond acceptors.
[d] Values for atom-based log of the partition coefficient (ALogP) from https://www.ebi.ac.uk/chembl/.
[e] PSA, polar surface area.
[f] Complexity values obtained from https://pubchem.ncbi.nlm.nih.gov/.
[g] Includes aromatic and nonaromatic rings.

6.2. The importance of lipophilicity and ligand efficiency

6.2.1. Lipophilic efficiency, LipE

After the emergence of Lipinski's Ro5 in 2001 [94], subsequent work on the physical and chemical properties of orally bioavailable medicines has led to various refinements [95–102]. For example, lipophilic efficiency, or LipE, is a property that is used in drug discovery and development that combines potency and lipophilic-driven binding as a strategy to increase binding efficacy. The following formulas are used to compute lipophilic efficiency:

$$\text{LipE} = \text{p}IC_{50} - \text{ALogP};\ \text{LipE} = \text{p}K_i - \text{ALogP}$$

Like its usage to express the molar hydrogen ion concentration as pH, the operator p denotes the negative of the Log_{10} of the IC_{50} or K_i. Furthermore, ALogP is an atom-based computed Log_{10} of the partition coefficient; this parameter denotes the ratio of the drug solubility in the organic phase divided by its solubility in the aqueous phase of immiscible *n*-octanol/water.

The second term of the equation (– ALogP or minus ALogP) reflects the lipophilicity of a medicinal and the value is computed using an algorithm based upon the properties of thousands of reference organic compounds. The more soluble a compound is in the organic phase when compared with the aqueous phase of a *n*-octanol/water mixture, the greater is its lipophilicity. Leeson and Springthorpe suggested that drug lipophilicity, as assessed by its – ALogP value, is one of the more important properties that should be monitored during drug development [96]. Their use of – ALogP was based upon experiments performed before the determination of the distribution coefficient (D) became more common. The distribution coefficient ($\text{LogD}_{7.4}$) is the ratio of the solubility of the ionized and un-ionized ligand in the organic phase over the aqueous phase of immiscible *n*-octanol/water at a specified pH of the aqueous phase, which is usually 7.4. For all intents and purposes, either ALogP or LogD can be used to monitor several compounds in the same study. Note that an agent with a substantial lipophilicity and a large negative (– ALogP) value decreases the lipophilic efficiency.

An elevated lipophilicity may facilitate the binding of an agent to adventitious targets that may increase toxicity leading to adverse events. One goal during drug development is to increase potency without simultaneously increasing lipophilicity. The use of lipophilic efficiency aids in the optimization of lead compounds by directly comparing a series of drug congeners; furthermore, the same procedure for determining the lipophilic efficiency should be used to ensure that such comparisons are sound [98,99]. To cite a cogent example, progress in the optimization of lead compounds during the development of crizotinib was monitored by using lipophilic efficiency as an index of binding effectiveness as described by Cui et al. [103]; crizotinib is FDA-approved for the management of ALK-positive and ROS1-positive NSCLC.

The ALogP of various agents can be calculated in a matter of minutes. Because experimental measurements of LogP are labor intensive, such determinations are carried out in only select cases. Hopkins et al. proposed that acceptable values for LogP are less than ~ 3 and those of lipophilic efficiency are greater than ~ 5 [98]. Increasing the potency and decreasing the lipophilicity during drug development generally produces drugs with improved pharmacological properties. The average value of lipophilic efficiency (LipE) for 69 FDA-approved small molecule protein kinase blockers (omitting the macrolides) is 4.36 with a range from 1.3 (neratinib) to 7.56 (tofacitinib) with a standard deviation of 1.49 (Table 9). The average value for ALogP for the 69 FDA-approved drugs (excluding the three macrolides) was 4.19 with a range from 1.1 (baricitinib) to 6.36 (nilotinib) with a standard deviation of 1.22.

6.2.2. Ligand efficiency, LE

The ligand efficiency (LE) relates potency, or binding affinity, to the number of heavy (nonhydrogen) atoms of a drug. The following formula is used to compute this property:

$$\text{LE} = \Delta G^{\circ\prime}/\text{N} = -\text{RT}\ \ln K_{eq}/\text{N} = -2{\cdot}303\text{RT}\ \text{Log}\ K_{eq}/\text{N}$$

$\Delta G^{\circ\prime}$ is the standard free energy change of a ligand binding to its target enzyme at neutral pH, R denotes the universal gas constant or energy-temperature coefficient (1.98×10^{-3} kcal/degree-mol), T represents the temperature in degrees Kelvin, K_{eq} is the value of the equilibrium constant, and N represents the number of heavy (nonhydrogen) atoms in the drug. The K_i or IC_{50} values represent surrogates for the equilibrium constant. At a physiological temperature of 37 °C (310 K), this equation becomes $-(2.303 \times (1.98 \times 10^{-3}/\text{K}) \times 310\ \text{K}\ \text{Log}\ K_{eq})/\text{N}$ or $-1.41\ \text{Log}\ K_{eq}/\text{N}$. Other investigators use a temperature of 300 K and the multiplication factor becomes – 1.37 [98,102]. Ligand efficiency reflects ligand affinities based upon the average binding energy per atom. Furthermore, ligand efficiency is quite helpful in fragment-based drug discovery protocols and, like lipophilic efficiency, it facilitates the selection of congeners of lead compounds for further development [99].

Ligand efficiency reflects the binding affinity per heavy atom of the ligand or drug of interest. The value of N is a surrogate for the molecular weight. The equation used to calculate ligand efficiency shows that its value is directly proportional to $-\text{Log}\ K_{eq}$ (a positive number), or the binding affinity, and is inversely proportional to the number of nonhydrogen atoms. Hopkins et al. indicated that optimal values for ligand efficiency (LE) should be greater than 0.3 kcal per mol per nonhydrogen atom [95,98]. Ligand efficiency values for the FDA-approved small molecule protein kinase blockers based upon representative K_i or IC_{50} values are included in Table 9. The average value for ligand efficiency for 69 of the FDA-approved protein kinase inhibitors (excluding the three macrolides) was 0.0.361 with a range from 0.237 (mobocertinib) to 0.558 (tofacitinib) and a standard deviation of 0.064. Five drugs had values of less than 0.3 including mobocertinib, midostaurin, neratinib, nilotinib, and the newly approved pacritinib. The values for ligand efficiency (LE) and lipophilic efficiency (LipE) listed in Table 9 are based on data acquired under different experimental conditions. Accordingly, these values cannot be used to make a direct comparison of the drugs because different procedures were used to obtain the data. These findings were acquired from various drug development projects and provide only representative values. The major protein kinase families that are targeted by the FDA-approved drugs are also listed in Table 9.

6.2.3. Additional chemical descriptors of orally effective drugs

To improve drug characteristics linked to oral effectiveness, not-unexpectedly, the Ro5 has generated many variations and corollaries. For example, Veber et al. reported that the polar surface area (PSA) and the number of rotatable bonds differentiates between orally active and inactive agents for a large series of compounds in rats [100]. They found that the optimal number of rotatable bonds is 10 or less. This property controls passive membrane permeation and mirrors molecular flexibility (degrees of freedom). Moreover, the number of degrees of freedom is related to the entropy change that results from ligand binding and determines in part the amount of drug binding to its targets. With the exceptions of four drugs with 11 rotatable bonds (erlotinib, fedratinib, lapatinib, neratinib) and mobocertinib with 13 rotatable bonds, the remaining 64 drugs (the macrolides were excluded) have 10 or fewer of

Table 9
Properties of FDA-approved small molecule protein kinases inhibitors[a].

Drug	Target, kinase family[b]	K_i nM[c]	pK_i	ALogP[d]	LipE[e]	N[f]	LE[g]	Dosage, mg/day[h]	Solubility, μg/ml[i]	Log $D_{7.4}$[c]	nRb[j]	nAr[k]	Benzenes	QED[l]
Abemaciclib	CDK4, S/T	0.6	9.22	4.94	4.28	37	0.351	400 *	15.9	3.76	7	4	0	0.38
Abrocitinib	JAK1, NRY	5.1	8.29	1.25	7.04	22	0.531	100	420	0.79	6	2	0	0.83
Acalbrutinib	BTK, NRY	3.1	8.51	3.31	5.20	35	0.343	200 *	10.9	2.56	4	4	1	0.45
Afatinib	EGFR, RY	0.5	9.33	4.39	4.94	34	0.387	40	12.8	2.34	8	3	1	0.46
Alectinib	ALK, RY	1.9	8.72	4.77	3.95	36	0.342	1200 *	10.5	4.75	3	3	0	0.58
Asciminib	BCR-Abl, NRY	0.5	9.3	3.46	5.84	31	0.300	80	55	3.86	6	4	1	0.50
Avapritinib	PDGFRα, RY	0.18	9.7	2.61	7.09	37	0.370	300	30.1	2.12	5	5	1	0.39
Axitinib	VEGFR2, RY	0.25	9.6	4.64	4.96	28	0.483	300	0.55	4.15	5	4	1	0.52
Baricitinib	JAK2, NRY	7	8.15	1.1	7.05	26	0.442	2	357	-0.19	5	3	0	0.72
Belumosudil	ROCK2, S/T	53.9	7.3	4.82	2.48	34	0.303	200	2.89	4.02	7	5	1	0.33
Binimetinib	MEK1, DS	12	7.92	3.01	4.91	27	0.414	90 *	49.9	3.81	6	3	1	0.40
Bosutinib	BCR-Abl, NRY	20	7.7	5.19	2.51	36	0.302	500	9.5	3.37	9	3	1	0.38
Brigatinib	ALK, RY	0.398	9.4	5.09	4.31	40	0.331	180	22	2.49	8	3	2	0.35
Cabozantinib	RET, RY	5	8.3	5.54	2.76	37	0.316	40	1.99	4.65	8	4	2	0.31
Capmatinib	MET, RY	0.13	9.89	3.43	6.46	31	0.450	800 *	5.29	2.96	5	5	1	0.49
Ceritinib	ALK, RY	0.2	9.7	6.36	3.34	38	0.360	750	2.22	3.38	9	3	2	0.28
Cobimetinib	MEK1, DS	0.79	9.1	3.78	5.32	30	0.428	60	42.2	2.73	4	2	2	0.53
Crizotinib	ALK, RY	0.63	9.2	5.04	4.16	30	0.432	500 *	6.11	0.95	5	3	1	0.53
Dabrafenib	B-Raf, S/T	0.4	9.4	5.36	4.04	35	0.379	300 *	3.27	5.10	6	4	2	0.37
Dacomitinib	EGFR, RY	2	8.7	5.16	3.54	33	0.372	45	8.74	3.53	7	3	1	0.47
Dasatinib	BCR-Abl, NRY	0.16	9.8	3.31	6.49	33	0.419	100	12.8	3.74	7	3	1	0.47
Encorafenib	B-Raf, S/T	0.3	9.52	3.91	5.61	36	0.373	450	11.2	2.61	10	3	1	0.37
Entrectinib	TRKA, RY	1	9	5.03	3.97	41	0.310	600	8.9	4.87	9	4	2	0.29
Erdafitinib	FGFR1, RY	2	8.7	4.18	4.52	33	0.372	8	13	1.25	11	4	1	0.41
Erlotinib	EGFR, RY	0.32	9.5	3.41	6.09	29	0.462	150	8.91	3.20	7	3	1	0.42
Everolimus	FKBP12/mTOR, S/T	?	?	6.2	?	68	?	10	1.63	7.40	9	0	0	0.13
Fedratinib	JAK2, NRY	6	8.22	4.82	3.40	37	0.313	400	9.49	3.23	11	3	2	0.35
Fostamatinib	Syk, RY	17	7.77	3.09	4.68	40	0.274	300 *	52	-0.52	10	3	1	0.26
Futibatinib	FGFR2, RY	4	8.4	1.78	6.62	31	0.382	20	40	1.54	4	6	1	0.51
Gefitinib	EGFR, RY	0.5	9.3	4.28	5.02	31	0.423	250	27	3.64	8	3	1	0.52
Gilteritinib	Flt3, RY	0.41	9.39	2.7	6.69	40	0.331	120	22.3	1.69	9	2	1	0.43
Ibrutinib	BTK, NRY	12.6	7.9	4.22	3.68	33	0.338	560	20.3	3.63	5	4	2	0.47
Imatinib	BCR-Abl, NRY	1	9	4.59	4.41	37	0.343	600	14.6	3.80	7	4	2	0.39
Infigratinib	FGFRs	5	8.3	5.35	2.95	38	0.308	125	29.9	3.99	8	3	2	0.38
Lapatinib	EGFR, RY	1	9	6.14	2.86	40	0.317	1250	22.3	4.40	11	5	2	0.18
Larotrectinib	TRK, RY	9.7	8.01	2.95	5.06	31	0.364	200 *	238	2.44	3	3	1	0.67
Lenvatinib	VEGFR2, RY	3.98	8.4	4.07	4.33	30	0.395	24	6.22	2.52	6	3	1	0.55
Lorlatinib	ALK, RY	9	8.05	2.8	5.25	30	0.378	100	108	1.62	0	3	1	0.61
Midostaurin	Flt3, RY	37	7.43	5.91	1.52	43	0.244	200 *	15.7	5.43	3	6	1	0.29
Mobocertinib	EGFR, RY	60	7.22	5.08	2.14	43	0.237	160	13.6	3.79	13	4	1	0.17
Neratinib	ErbB2/HER2, RY	59	7.23	5.93	1.30	40	0.255	240	6.74	3.05	11	4	1	0.22
Netarsudil	ROCK1/2, S/T	1	9	4.89	4.11	34	0.373	0.01	0.23	3.42	8	4	2	0.39
Nilotinib	BCR-Abl, NRY	12.5	7.9	6.36	1.54	39	0.286	600 *	2.01	5.35	6	5	2	0.27
Nintedanib	FGFR, RY	39.8	7.4	3.62	3.78	40	0.261	300 *	30.9	2.57	8	4	2	0.35
Osimertinib	EGFR, RY	7	8.15	4.51	3.64	37	0.311	80	22.4	3.01	10	4	1	0.31
Pacritinib	JAK2, NRY	19	7.72	4.96	2.21	35	0.289	100	38	3.11	4	4	2	0.54
Palbociclib	CDK4, S/T	10	8	2.97	5.03	33	0.342	125	17.4	1.30	5	3	0	0.58
Pazopanib	VEGFR2, RY	30	7.52	3.14	4.38	31	0.342	800	43.3	3.55	5	4	1	0.49
Pemigatinib	FGFR, RY	0.5	9.3	3.66	5.64	35	0.375	13.5	144	1.80	6	3	1	0.57
Pexidartinib	CSF1R, RY	13	7.89	5.23	2.66	29	0.384	800 *	3.15	4.55	5	4	0	0.47
Ponatinib	BCR-Abl, NRY	1	9	4.46	4.54	39	0.325	45	2.95	4.54	8	4	2	0.39
Pralsetinib	RET	0.5	9.3	4.2	5.10	39	0.336	400	10.1	3.64	6	4	0	0.31
Regorafenib	VEGFR2, RY	4.2	8.4	5.69	2.71	33	0.359	160	1.02	4.49	5	3	2	0.41
Ribociclib	CDK4, S/T	10	8	2.8	5.20	32	0.353	600	231	0.91	5	3	1	0.64
Ripretinib	RET	3	8.52	5.67	2.85	33	0.364	150	5.83	4.38	5	4	2	0.32
Ruxolitinib	JAK1, NRY	1.2	8.92	3.47	5.45	23	0.547	20 *	116	2.48	4	3	0	0.8
Selpercatinib	RET, RY	1	9	3.28	5.72	39	0.325	320 *	29.9	3.11	8	4	0	0.37
Selumetinib	MEK1, DS	14	7.85	3.53	4.32	27	0.410	80 *	21	4.27	6	3	1	0.39
Sirolimus	FKBP12/mTOR, S/T	?	?	6.18	?	65	?	2	1.73	7.45	6	0	0	0.16
Sorafenib	VEGFR1, RY	15.8	7.8	5.55	2.25	32	0.344	800 *	1.71	4.34	5	3	2	0.46
Sunitinib	VEGFR2, RY	3.98	8.4	3.33	5.07	29	0.408	50	30.8	1.28	7	2	0	0.63
Temsirolimus	FKBP12/mTOR, S/T	?	?	4.39	?	73	?	25 * *	2.35	?	7	0	0	?
Tepotinib	MET, RY	1	9	4.01	4.99	37	0.343	450	?	2.26	6	4	2	0.38
Tivozanib	VEGFR2	6.5	8.19	5.64	2.55	37	0.312	1.34	52.1	4.16	11	4	1	0.39
Tofacitinib	JAK1, NRY	0.79	9.1	1.54	7.56	23	0.558	10 *	299	1.19	3	2	0	0.93
Trametinib	MEK1, DS	3.4	8.47	3.94	4.53	37	0.323	2	30.7	3.18	5	3	2	0.33
Trilaciclib	CDK4/6, S/T	1	9	2.72	6.28	33	0.385	480	260	2.29	3	3	0	0.64
Tucatinib	ErbB2/HER2, RY	8	8.1	5.09	3.01	36	0.317	600 *	4	5.25	6	5	1	0.36
Upadacitinib	JAK1, NRY	43	7.37	2.91	4.46	27	0.385	15	70.7	0.85	3	3	0	0.73
Vandetanib	RET, RY	50	7.3	5	2.30	30	0.343	300	10.2	2.81	6	3	1	0.54
Vemurafenib	B-Raf, S/T	3.98	8.4	5.54	2.86	33	0.359	1920 *	0.36	4.61	7	4	2	0.33
Zanubrutinib	BTK, NRY	0.3	9.52	4.22	5.30	35	0.384	320 *	10.3	3.42	6	3	2	0.52

[a] Drugs previously not reviewed (Refs. [10–13]) are given in **bold** type.
[b] NRY, non-receptor protein-tyrosine kinase; RY, receptor protein-tyrosine kinase; S/T, protein-serine/threonine kinase; DS; dual specificity protein kinase (catalyzes protein-tyrosine and then threonine phosphorylation of target kinase activation segments but evolutionarily in the protein-serine/threonine kinase family).
[c] Representative values obtained from www.ebi.ac.ug/chembl/ and from klifs.net.
[d] Values for atom-based ALogP from https://www.ebi.ac.uk/chembl/
[e] LipE = pIC$_{50}$ – ALogP
[f] N, Number of heavy (nonhydrogen) atoms.
[g] LE = – 2.303 RT Log$_{10}$ K_i/N where N is the number of heavy (non-hydrogen) atoms in the drug.
[h] Dosage from FDA label; * , one-half of total daily dose taken twice per day; * *, once weekly.
[i] Values from https://go.drugbank.com/drugs/
[j] nRb, number of Rotatable bonds.
[k] nAr, number of Aromatic rings.
[l] QED, summed, weighted desirability (scores using MW + ALogP + HBD + HBA + PSA + nRotB + nAr) obtained from https://www.ebi.ac.uk/chembl/; see Ref. [102] for a full explanation.

these bonds. The average value is 6.46 and the number of rotatable bonds ranges from 0 (lorlatinib) to 13 (mobocertinib). Moreover, Veber et al. found that drugs with a polar surface area less than or equal to 140 Å^2 are orally bioavailable [100]. This variable represents the sum of the surface over all polar atoms, primarily oxygen and nitrogen, but it also includes any connected hydrogen atoms. Excluding the three macrolides, the average value for the surface area is 97.8 Å^2 with a range from 59.5 (vandetanib) to 187 (neratinib). Abemaciclib, pexidartinib, and neratinib are the only drugs with a polar surface area exceeding 140 Å^2 (Table 8). Additionally, Oprea reported that the number of ring structures (both aromatic and nonaromatic) in most orally approved drugs is three or greater [101]. All approved small molecule protein kinase blockers have three or more rings with an average value of 4.32 and a range from three to six. Except for temsirolimus and trilaciclib (which are given intravenously) and netarsudil (an eye drop), all of the FDA-approved drugs listed are orally bioavailable. Moreover, ruxolitinib is effective orally and topically.

The molecular complexity of a compound is based upon the elements it contains, its structural features, and its symmetry. The complexity is calculated with the Bertz/Hendrickson/Ihlenfelt rules [104,105]. It is based upon the number and identity of the constituent atoms, the bonding pattern, and the type of the chemical bonds (single, double, triple, aromatic). Molecular complexity ranges from 0 for simple ions to several thousand for intricate natural products. Larger chemicals usually have a greater molecular complexity value than smaller ones. In contrast, substances containing few diverse elements and those that are highly symmetrical possess a smaller molecular complexity value. The molecular complexity values for the drugs in this article were acquired from PubChem (https://pubchem.ncbi.nlm.nih.gov/). For the 72 FDA-approved kinase inhibitors, the mean complexity value is 765 with a range from 453 (pralsetinib) to 2010 (temsirolimus) (Table 8). As anticipated, the three large macrolide compounds possess the greatest molecular complexity values. There are no optimal or recommended molecular complexity values for orally effective drugs; however, this parameter may be helpful in predicting the ease or difficulty of drug synthesis, an important consideration in the commercial production of pharmaceutical agents.

Leeson et al. compared drug properties in two time frames: 1990–2009 and 2010–2020 [102]. They found that the lipophilicity and molecular weight of approved drugs increased with time. We compared the averages of selected properties of FDA-approved protein kinase antagonists during two-time frames: 2001 – 2011 and 2012 – 2022. This analysis excluded the three large macrolides. The average molecular weight increased from 459 to 482 during this period as well as the heavy atom count (32.3–34.6), the polar surface area (93.8–98.6 Å^2), and molecular complexity (661−730). However, the average number of hydrogen bond donors and acceptors, the ALopP, the number of rotatable bonds, the ring count, ligand efficiency, lipophilic efficiency, and the potency (K_i values) were essentially unchanged (Tables 8 and 9). Leeson et al. reported that the molecular weight of all approved drugs, including protein kinase antagonists, has increased over time [102].

Ritchie and Macdonald examined the application of aromaticity in the drug development process [106]. Aromaticity refers to cyclically conjugated compounds with a stability that is significantly greater than a localized Kekulé structure owing to electron delocalization. They considered bicyclic and tricyclic structures as containing two and three aromatic rings, respectively. The aromatic ring count refers to structures containing carbon and heteroatom components. These investigators reported that increasing the number of carboaromatic rings had a detrimental effect on pharmacologic effectiveness by decreasing aqueous solubility, increasing binding to serum albumin, and inhibiting CYP450 (cytochrome P450). We find that the average number of aromatic rings in the 72-approved protein kinase antagonists was 3.28 and the mean number of benzene moieties was 1.00. All of the FDA-approved kinase blockers with the exception of the three macrolides have a least two aromatic rings; furthermore, midostaurin had the largest number of rings at six. Fifteen of the drugs lacked benzene fragments and the number of drugs possessing one or two benzenes was about evenly distributed among the remainder (Table 9).

Bayliss et al. evaluated the lipophilicity, dose, and solubility for oral drug and oral drug candidates [107]. They summarized observations indicating that daily doses of 100 mg or less reduces the risk of toxicity. The range of dosages for protein kinase blockers given orally is from 1.34 mg to 1920 mg daily with an average of about 300 mg. The daily doses range from 1.34, 2, and 2 mg for tivozanib, trametinib, and baricitinib and 1200, 1250, and 1920 mg for alectinib, lapatinib, and vemurafenib, respectively. Only 22 of the bioavailable kinase inhibitors have doses of 100 mg or less. Bayliss et al. reported that agents with a solubility in water of 100 μg/ml or less are associated with increased risk of failure during clinical trials and drug development [107]. We tallied the solubility of the approved protein kinase antagonists in water and found a range from 0.36 μg/ml (vemurafenib) to 420 μg/ml for the newly approved abrocitinib with a mean value of about 45 μg/ml. The range in solubilities and dosages among the FDA-approved drugs is nearly three orders of magnitude.

7. Epilogue and perspective

The work of Meharena et al. identified three shell residues in murine protein kinase A that strengthen and stabilize the regulatory spine and are important in supporting catalytic activity [31]. Although we surmise that comparable residues in other protein kinases perform the same functions, it would be advantageous to have experimental evidence to support or refute this notion. We also surmise that drugs that extend into the back pocket of their target enzymes have longer residence times than drugs that do not enter the back pocket [32] and it would be helpful to have additional experimental evidence to support this hypothesis. Information on the frequency of acquired resistance to protein kinase inhibitors used for the management of inflammatory diseases would also be helpful.

Although considerable progress has been made in the discovery and development of small molecule protein kinase inhibitors since the FDA-

approval of imatinib in 2001, this field is in its early stages. Oprea et al. hypothesized that the increased expression of many understudied protein kinases may play an important role in tumorigenesis [108]. Furthermore, these understudied proteins may be effective drug targets. Examples include cyclin-dependent protein kinase 12 (CDK12), eukaryotic elongation factor 2 kinase (EEF2K), and mitogen-activated protein kinase kinase kinase 1 (MAP3K1). Most of the FDA-approved kinase antagonists are antineoplastic and others function as immunomodulators [10, 109–111]. Owing to the inherent genetic changes in neoplastic cells, resistance to protein kinase inhibitors occurs on a *nearly* universal basis. This resistance promoted the development of second, third, and later generation inhibitors that target the same enzyme and disease. Furthermore, acquired drug resistance is frequently the product of gatekeeper mutations in the initial protein kinase target [3]. A gatekeeper mutation in *EGFR* (*T790M*) represents a case in point and this is the third most commonly observed protein kinase mutation. Moreover, it is responsible for about half of all acquired *EGFR* inhibitor resistance mutations. Although inflammation per se is not associated with the degree of genetic instability observed in neoplastic diseases, it is unclear whether acquired resistance arises during the management of inflammatory disorders.

Because 244 protein kinase genes map to disease loci or cancer amplicons [8], it is probable that (i) a significant increase in the number of drugs blocking additional protein kinases will be discovered and (ii) new medications will be developed for the treatment of additional illnesses [112–115]. Adding new protein kinase targets to the therapeutic armamentarium will require the elucidation of signaling pathways and networks in addition to the RAS-Raf-MEK MAP kinase and phosphatidylinositol 3-kinase-AKT signaling modules [116]. Along with the 72 approved protein kinase blockers considered in this article, the FDA has approved five drugs that inhibit phosphatidylinositol 3-kinases (PI 3-kinases are members of the atypical protein kinase family) [9]. These include alpelisib – an orally bioavailable PI 3-kinase-α inhibitor that is used for the treatment of breast cancer – and umbralisib, duvelisib, copanlisib, and idelalisib that are orally effective PI 3-kinase-δ inhibitors that are approved for the third-line treatment of follicular lymphomas and other hematological disorders. As the protein kinase inhibitor field develops, it is likely that protein kinase blockers with new chemotypes, pharmacophores, and scaffolds will be formulated [117]. The newly discovered asciminib is a unique type IV allosteric inhibitor because it binds directly to its drug target. The three macrolides are type IV allosteric inhibitors that bind to FKBP12 and the drug-protein complex inhibits the catalytic activity of mTOR; these three drugs are indirect blockers of their target protein kinase [118]. One can expect that additional allosteric inhibitors will be found that block novel enzymes that are part of a range of protein kinase signal transduction modules [119]. Moreover, it is probable that new irreversible inhibitors that target protein kinases with –SH groups near the ATP-binding site will be forthcoming.

Of the 72 FDA-approved drugs, receptor protein-tyrosine kinase are the chief targets of 40 of them followed by nonreceptor protein-tyrosine kinases (16), protein-serine/threonine kinases (12), and dual-specificity protein kinases (4) (Table 10). Members of the EGFR/ErbB family represent the top-ranked targets followed by the VEGFR, JAK, BCR-Abl, ALK, and FGFR families. CDK4/6 is targeted by four of the FDA-approved inhibitors that are prescribed for the management of breast cancer. The dual specificity (MEK1/2) protein kinases, which block the RAS-Raf-MEK MAP kinase pathway, include binimetinib (used in combination with encorafenib for the treatment of melanoma), cobimetinib (used in combination with vemurafenib for the treatment of melanoma), selumetinib (prescribed for neurofibromatosis I or Von Recklinghausen disease) and trametinib (prescribed for melanoma and NSCLC).

The clinical efficacy of drugs that are FDA-approved for the treatment of CML is vastly superior to other protein kinase inhibitors that are used in the management of other disorders. Patients with chronic myelogenous leukemia treated with BCR-Abl blockers have an annual mortality rate of 0.5% or less when compared with age-matched normal groups [120,121]. Imatinib (first generation), bosutinib, dasatinib, and nilotinib (second generation) have been approved by the FDA for frontline therapy while ponatinib (third generation) is approved for resistant disease with a *T315I* mutation or after failure with at least two other protein-tyrosine kinase inhibitors [122]. Asciminib is a STAMP (specifically targeting the Abl myristoyl pocket) inhibitor approved as a first-line treatment in patients with the *T315I* mutation and as a third-line treatment for CML [91]. Pre-clinical (animal) studies demonstrate that the use of asciminib with an antagonist targeting the Abl-1 ATP-binding site prevents the emergence of drug-resistance to either asciminib or the ATP-competitive antagonists. Several clinical trials using the combination of asciminib with bosutinib, imatinib, or nilotinib are now underway (ClinicalTrials.gov).

Table 10
Principal FDA-approved protein kinase inhibitor drug targets[a].

Kinase family	No.	Class of Kinase	RY	NRY	S/T	Y/T
ErbB	9	RY	9			
VEGFR	8	RY	8			
JAK	7	NRY		7		
BCR-Abl	6	NRY		6		
ALK	5	RY	5			
FGFR	5	RY	5			
CDK4/6	4	S/T			4	
MEK1/2	4	Y/T				4
B-Raf	3	S/T			3	
BTK	3	NRY		3		
FKBP	3	S/T			3	
MET	3	RY	3			
Flt3	2	RY	2			
RET	2	RY	2			
ROCK	2	S/T			2	
TRKA	2	RY	2			
CSF1	1	RY	1			
Kit	1	RY	1			
PDGFR	1	RY	1			
Syk	1	RY	1			
	72		40	16	12	4

[a] NYR, nonreceptor protein-tyrosine kinase; RY, receptor protein-tyrosine kinase; S/T, protein-serine/threonine kinase; Y/T, Dual specificity protein kinase – tyrosine phosphorylation followed by threonine phosphorylation of target kinase activation segments.

The aims of the current management of CML are to promote patient survival and to attain treatment-free remission (TFR), whenever possible. For promoting survival, frontline treatment with imatinib, dasatinib, bosutinib, or nilotinib are all effective. If imatinib therapy is used for frontline treatment, a change in therapy at the first indication of resistant disease is now standard practice. One reason for initially using imatinib is its availability as a generic agent at a cost lower than that of other drugs. The choice of the second line treatment is guided by an assessment of possible mutations of the Abl kinase domain and by the patient's age and co-morbidities [121]. Side effects produced by bosutinib include diarrhea (10–30%, which is mild and self-limited) and kidney and liver dysfunction. Dasatinib can produce occasional pulmonary hypertension (1–2%), pleural effusions (10–15%), and myelosuppression (10–20%). Nilotinib can lead to hyperglycemia (10–15%), exacerbate diabetes mellitus (5–10%), and produce pancreatitis (1–3%). Ponatinib produces the most serious side effects including vasospastic disease (10–15%), hypertension (20–30%), skin rashes (5–10%), and pancreatitis (5%) [121].

Attaining treatment-free (TFR) remission is desirable in younger patients in order to avoid lifelong therapy. A deep molecular response (DMR), which is defined as a 4–4.5 log reduction in the BCR-Abl-1 transcripts on the International Scale (the ratio of BCR-Abl1 transcripts to Abl1 transcripts), is one criterion for discontinuing drug treatment. Discontinuing therapy after a deep molecular response lasting two-to-three years is coupled with a treatment-free remission rate of

50–60%. When therapy is discontinued after five years of a deep molecular response, the probability of achieving a treatment-free remission rate is greater than 80%. When remission is not achieved, patients fortunately respond to the therapy given before drug withdrawal. For additional information on protocols for producing treatment-free remission, see Refs. [121,123,124]. The concept of treatment-free remission for CML was unthinkable at the beginning of the targeted protein kinase therapy era. In the first decade of the 21st century, the idea that drug treatment for CML could be discontinued and the disease would remain abated was a pipedream.

Conflict of interest

The author is unaware of any affiliations, memberships, or financial holdings that might be perceived as affecting the objectivity of this review.

Data Availability

No data was used for the research described in the article.

Acknowledgments

I thank Dr. Albert J. Kooistra for providing the template depicted in Fig. 3 and Laura M. Roskoski for providing editorial and bibliographic assistance. I also thank Jasper Martinsek and Josie Rudnicki for their help in preparing the figures and W.S. Sheppard and Pasha Brezina for their help in structural analyses. The colored figures in this paper were evaluated to ensure that their perception was accurately conveyed to colorblind readers [125].

Appendix A. Supporting information

Supplementary data associated with this article can be found in the online version at doi:10.1016/j.phrs.2022.106552.

References

[1] P. Cohen, Protein kinases – the major drug targets of the twenty-first century? Nat. Rev. Drug Discov. 1 (2002) 309–315, https://doi.org/10.1038/nrd773.
[2] R. Roskoski Jr., A historical overview of protein kinases and their targeted small molecule inhibitors, Pharm. Res. 100 (2015) 1–23, https://doi.org/10.1016/j.phrs.2015.07.010.
[3] P. Cohen, D. Cross, P.A. Jänne, Kinase drug discovery 20 years after imatinib: progress and future directions, Nat. Rev. Drug Discov. 20 (2021) 551–569, https://doi.org/10.1038/s41573-021-00195-4.
[4] M.M. Attwood, D. Fabbro, A.V. Sokolov, S. Knapp, H.B. Schiöth, Trends in kinase drug discovery: targets, indications and inhibitor design, Nat. Rev. Drug Discov. 20 (2021) 839–861, https://doi.org/10.1038/s41573-021-00252-y. Author correction. Nat Rev Drug Discov 2021;20:798. doi: 10.1038/s41573-021-00303-4.
[5] G.K. Kanev, C. de Graaf, I.J.P. de Esch, R. Leurs, T. Würdinger, B.A. Westerman, A.J. Kooistra, The landscape of atypical and eukaryotic protein kinases, Trends Pharm. Sci. 40 (2019) 818–832, https://doi.org/10.1016/j.tips.2019.09.002.
[6] F. Carles, S. Bourg, C. Meyer, P. Bonnet, PKIDB: a curated, annotated and updated database of protein kinase inhibitors in clinical trials, Molecules 23 (2018), E908, https://doi.org/10.3390/molecules23040908.
[7] P.M. Fischer, Approved and experimental small-molecule oncology kinase inhibitor drugs: a mid-2016 overview, Med. Res. Rev. 37 (2017) 314–367, https://doi.org/10.1002/med.21409.
[8] G. Manning, D.B. Whyte, R. Martinez, T. Hunter, S. Sudarsanam, The protein kinase complement of the human genome, Science 298 (2002) 1912–1934, https://doi.org/10.1126/science.1075762.
[9] R. Roskoski Jr., Properties of FDA-approved small molecule phosphatidylinositol 3-kinase inhibitors prescribed for the treatment of malignancies, Pharm. Res. 168 (2021), 105579, https://doi.org/10.1016/j.phrs.2021.105579.
[10] R. Roskoski Jr., Properties of FDA-approved small molecule protein kinase inhibitors, Pharm. Res. 144 (2019) 19–50, https://doi.org/10.1016/j.phrs.2019.03.006.
[11] R. Roskoski Jr., Properties of FDA-approved small molecule protein kinase inhibitors: a 2020 update, Pharm. Res. 152 (2020), 104609, https://doi.org/10.1016/j.phrs.2019.104609.
[12] R. Roskoski Jr., Properties of FDA-approved small molecule protein kinase inhibitors: a 2021 update, Pharm. Res. 165 (2021), 105463, https://doi.org/10.1016/j.phrs.2021.105463.
[13] R. Roskoski Jr., Properties of FDA-approved small molecule protein kinase inhibitors: a 2022 update, Pharm. Res. 175 (2022), 106037, https://doi.org/10.1016/j.phrs.2021.106037.
[14] S.H. Myers, V.G. Brunton, A. Unciti-Broceta, AXL inhibitors in cancer: a medicinal chemistry perspective, J. Med. Chem. 59 (2016) 3593–3608, https://doi.org/10.1021/acs.jmedchem.5b01273.
[15] B.L. Roth, D.J. Sheffler, W.K. Kroeze, Magic shotguns versus magic bullets: selectively non-selective drugs for mood disorders and schizophrenia, Nat. Rev. Drug Discov. 3 (2004) 353–359, https://doi.org/10.1038/nrd1346.
[16] R. Roskoski Jr., Orally effective FDA-approved protein kinase targeted covalent inhibitors (TCIs), Pharm. Res. 165 (2021), 105422, https://doi.org/10.1016/j.phrs.2021.105422.
[17] D.R. Knighton, J.H. Zheng, L.F. Ten Eyck, V.A. Ashford, N.H. Xuong, S.S. Taylor, J.M. Sowadski, Crystal structure of the catalytic subunit of cyclic adenosine monophosphate-dependent protein kinase, Science 253 (1991) 407–414, https://doi.org/10.1126/science.1862342.
[18] A.P. Kornev, S.S. Taylor, Dynamics-driven allostery in protein kinases, Trends. Biochem. Sci. 40 (2015) 628–647, https://doi.org/10.1016/j.tibs.2015.09.002.
[19] S.S. Taylor, J. Wu, J.G.H. Bruystens, J.C. Del Rio, T.W. Lu, A.P. Kornev, L.F. Ten Eyck, From structure to the dynamic regulation of a molecular switch: A journey over 3 decades, J. Biol. Chem. 296 (2021), 100746, https://doi.org/10.1016/j.jbc.2021.100746.
[20] R. Roskoski Jr., Cyclin-dependent protein serine/threonine kinase inhibitors as anticancer drugs, Pharm. Res. 139 (2019) 471–488, https://doi.org/10.1016/j.phrs.2018.11.035.
[21] R. Roskoski Jr., Hydrophobic and polar interactions of FDA-approved small molecule protein kinase inhibitors with their target enzymes, Pharm. Res. 169 (2021), 105660, https://doi.org/10.1016/j.phrs.2021.105660.
[22] S.K. Hanks, T. Hunter, Protein kinases 6. The eukaryotic protein kinase superfamily: kinase (catalytic) domain structure and classification, FASEB J. 9 (1995) 576–596.
[23] Madhusudan, E.A. Trafny, N.H. Xuong, J.A. Adams, L.F. Ten Eyck, S.S. Taylor, J. M. Sowadski, cAMP-dependent protein kinase: crystallographic insights into substrate recognition and phosphotransfer, Protein Sci. 3 (1994) 176–187, https://doi.org/10.1002/pro.5560030203.
[24] J. Zhou, J.A. Adams, Participation of ADP dissociation in the rate-determining step in cAMP-dependent protein kinase, Biochemistry 36 (1997) 15733–15738, https://doi.org/10.1021/bi971438n.
[25] P.A. Schwartz, B.W. Murray, Protein kinase biochemistry and drug discovery, Bioorg. Chem. 39 (2011) 192–210, https://doi.org/10.1016/j.bioorg.2011.07.004.
[26] A.P. Kornev, S.S. Taylor, Defining the conserved internal architecture of a protein kinase, Biochim. Biophys. Acta. 1804 (2010) 440–444, https://doi.org/10.1016/j.bbapap.2009.10.017.
[27] V. Modi, R.L. Dunbrack Jr., Defining a new nomenclature for the structures of active and inactive kinases, Proc. Natl. Acad. Sci. USA 116 (2019) 6818–6827, https://doi.org/10.1073/pnas.1814279116.
[28] V. Modi, R.L. Dunbrack Jr., Kincore: a web resource for structural classification of protein kinases and their inhibitors, Nucleic Acids Res. 50 (2022) D654–D664, https://doi.org/10.1093/nar/gkab920.
[29] A.P. Kornev, N.M. Haste, S.S. Taylor, L.F. Eyck, Surface comparison of active and inactive protein kinases identifies a conserved activation mechanism, Proc. Natl. Acad. Sci. USA 103 (2006) 17783–17788, https://doi.org/10.1073/pnas.0607656103.
[30] A.P. Kornev, S.S. Taylor, L.F. Ten Eyck, A helix scaffold for the assembly of active protein kinases, Proc. Natl. Acad. Sci. USA 105 (2008) 14377–14382, https://doi.org/10.1073/pnas.0807988105.
[31] H.S. Meharena, P. Chang, M.M. Keshwani, K. Oruganty, A.K. Nene, N. Kannan, S. S. Taylor, A.P. Kornev, Deciphering the structural basis of eukaryotic protein kinase regulation, PLoS Biol. 11 (2013), e1001690, https://doi.org/10.1371/journal.pbio.1001680.
[32] R. Roskoski Jr., Classification of small molecule protein kinase inhibitors based upon the structures of their drug-enzyme complexes, Pharm. Res. 103 (2016) 26–48, https://doi.org/10.1016/j.phrs.2015.10.021.
[33] R. Roskoski Jr., Anaplastic lymphoma kinase (ALK): structure, oncogenic activation, and pharmacological inhibition, Pharm. Res. 68 (2013) 68–94, https://doi.org/10.1016/j.phrs.2012.11.007.
[34] R. Roskoski Jr., Anaplastic lymphoma kinase (ALK) inhibitors in the treatment of ALK-driven lung cancers, Pharm. Res. 117 (2017) 343–356, https://doi.org/10.1016/j.phrs.2017.01.007.
[35] R. Roskoski Jr., The preclinical profile of crizotinib in the treatment of non-small cell lung cancer and other neoplastic disorders, Expert Opin. Drug Dis. 8 (2013) 1165–1179, https://doi.org/10.1517/17460441.2013.813015.
[36] R. Roskoski Jr., The ErbB/HER family of protein-tyrosine kinases and cancer, Pharm. Res. 79 (2014) 34–74, https://doi.org/10.1016/j.phrs.2013.11.002.
[37] R. Roskoski Jr., ErbB/HER protein-tyrosine kinases: structure and small molecule inhibitors, Pharm. Res. 87 (2014) 42–59, https://doi.org/10.1016/j.phrs.2014.06.001.
[38] R. Roskoski Jr., Small molecule inhibitors targeting the EGFR/ErbB family of protein-tyrosine kinases in human cancers, Pharm. Res. 139 (2019) 395–411, https://doi.org/10.1016/j.phrs.2018.11.014.

[39] R. Roskoski Jr., The role of small molecule platelet-derived growth factor receptor (PDGFR) inhibitors in the treatment of neoplastic disorders, Pharm. Res. 129 (2018) 65–83, https://doi.org/10.1016/j.phrs.2018.01.021.
[40] R. Roskoski Jr., The role of fibroblast growth factor receptor (FGFR) protein-tyrosine kinase inhibitors in the treatment of cancers including those of the urinary bladder, Pharm. Res. 151 (2020), 104567, https://doi.org/10.1016/j.phrs.2019.104567.
[41] R. Roskoski Jr., The role of small molecule Kit protein-tyrosine kinase inhibitors in the treatment of neoplastic disorders, Pharm. Res. 133 (2018) 35–52, https://doi.org/10.1016/j.phrs.2018.04.020.
[42] R. Roskoski Jr, A. Sadeghi-Nejad, Role of RET protein-tyrosine kinase inhibitors in the treatment RET-driven thyroid and lung cancers, Pharm. Res. 128 (2018) 1–17, https://doi.org/10.1016/j.phrs.2017.12.021.
[43] R. Roskoski Jr., Vascular endothelial growth factor (VEGF) and VEGF receptor inhibitors in the treatment of renal cell carcinomas, Pharm. Res. 120 (2017) 116–132, https://doi.org/10.1016/j.phrs.2017.03.010.
[44] R. Roskoski Jr., ROS1 protein-tyrosine kinase inhibitors in the treatment of ROS1 fusion protein-driven non-small cell lung cancers, Pharm. Res. 121 (2017) 202–212, https://doi.org/10.1016/j.phrs.2017.04.022.
[45] R. Roskoski Jr., The role of small molecule Flt3 receptor protein-tyrosine kinase inhibitors in the treatment of Flt3-positive acute myelogenous leukemias, Pharm. Res. 155 (2020), 104725, https://doi.org/10.1016/j.phrs.2020.104725.
[46] R. Roskoski Jr., Targeting BCR-Abl in the treatment of Philadelphia-chromosome positive chronic myelogenous leukemia, Pharm. Res. 178 (2022), 106156, https://doi.org/10.1016/j.phrs.2022.106156.
[47] R. Roskoski Jr., Janus kinase (JAK) inhibitors in the treatment of inflammatory and neoplastic diseases, Pharm. Res. 111 (2016) 784–803, https://doi.org/10.1016/j.phrs.2016.07.038.
[48] R. Roskoski Jr., Janus kinase (JAK) inhibitors in the treatment of neoplastic and inflammatory disorders, Pharm. Res. 183 (2022), 106362, https://doi.org/10.1016/j.phrs.2022.106362.
[49] R. Roskoski Jr., Ibrutinib inhibition of Bruton protein-tyrosine kinase (BTK) in the treatment of B cell neoplasms, Pharm. Res. 113 (2016) 395–408, https://doi.org/10.1016/j.phrs.2016.09.011.
[50] R. Roskoski Jr., Src protein-tyrosine kinase structure, mechanism, and small molecule inhibitors, Pharm. Res. 94 (2015) 9–25, https://doi.org/10.1016/j.phrs.2015.01.003.
[51] M.C. Frame, R. Roskoski Jr., Src family tyrosine kinases. Reference Module in life Sciences, Elsevier, Amsterdam, 2017, pp. 1–11, https://doi.org/10.1016/B978-0-12-809633-8.07199-5.
[52] R. Roskoski Jr., MEK1/2 dual-specificity protein kinases: structure and regulation, Biochem. Biophys. Res. Commun. 417 (2012) 5–10, https://doi.org/10.1016/j.bbrc.2011.11.145.
[53] R. Roskoski Jr., Allosteric MEK1/2 inhibitors including cobimetanib and trametinib in the treatment of cutaneous melanomas, Pharm. Res. 117 (2017) 20–31, https://doi.org/10.1016/j.phrs.2016.12.009.
[54] R. Roskoski Jr., Cyclin-dependent protein kinase inhibitors including palbociclib as anticancer drugs, Pharm. Res. 107 (2016) 249–275, https://doi.org/10.1016/j.phrs.2016.03.012.
[55] R. Roskoski Jr., ERK1/2 MAP kinases: structure, function, and regulation, Pharm. Res. 66 (2012) 105–143, https://doi.org/10.1016/j.phrs.2012.04.005.
[56] R. Roskoski Jr., Targeting ERK1/2 protein-serine/threonine kinases in human cancers, Pharm. Res. 142 (2019) 151–168, https://doi.org/10.1016/j.phrs.2019.01.039.
[57] R. Roskoski Jr., Targeting oncogenic Raf protein-serine/threonine kinases in human cancers, Pharm. Res. 135 (2018) 239–258, https://doi.org/10.1016/j.phrs.2018.08.013.
[58] R. Roskoski Jr., RAF protein-serine/threonine kinases: structure and regulation, Biochem. Biophys. Res. Commun. 399 (2010) 313–317, https://doi.org/10.1016/j.bbrc.2010.07.092.
[59] Y. Liu, K. Shah, F. Yang, L. Witucki, K.M. Shokat, A molecular gate which controls unnatural ATP analogue recognition by the tyrosine kinase v-Src, Bioorg. Med. Chem. 6 (1998) 1219–1226, https://doi.org/10.1016/s0968-0896(98)00099-6.
[60] A.C. Dar, K.M. Shokat, The evolution of protein kinase inhibitors from antagonists to agonists of cellular signaling, Annu Rev. Biochem. 80 (2011) 769–795, https://doi.org/10.1146/annurev-biochem-090308-173656.
[61] P.M. Ung, R. Rahman, A. Schlessinger, Redefining the protein kinase conformational space with machine learning, e2, Cell Chem. Biol. 25 (2018) 916–924, https://doi.org/10.1016/j.chembiol.2018.05.002.
[62] R. Hu, H. Xu, P. Jia, Z. Zhao, KinaseMD: kinase mutations and drug response database, Nucleic Acids Res. 49 (D1) (2021) D552–D561, https://doi.org/10.1093/nar/gkaa945.
[63] F. Zuccotto, E. Ardini, E. Casale, M. Angiolini, Through the "gatekeeper door": exploiting the active kinase conformation, J. Med. Chem. 53 (2010) 2691–2694, https://doi.org/10.1021/jm901443h.
[64] L.K. Gavrin, E. Saiah, Approaches to discover non-ATP site inhibitors, Med. Chem. Commun. 4 (2013) 41–51.
[65] V. Lamba, I. Ghosh, New directions in targeting protein kinases: focusing upon true allosteric and bivalent inhibitors, Curr. Pharm. Des. 18 (2012) 2936–2945, https://doi.org/10.2174/138161212800672813.
[66] J.J. Liao, Molecular recognition of protein kinase binding pockets for design of potent and selective kinase inhibitors, J. Med. Chem. 50 (2007) 409–424, https://doi.org/10.1021/jm0608107.
[67] O.P. van Linden, A.J. Kooistra, R. Leurs, I.J. de Esch, C. de Graaf, KLIFS: a knowledge-based structural database to navigate kinase-ligand interaction space, J. Med. Chem. 57 (2014) 249–277, https://doi.org/10.1021/jm400378w.
[68] A.J. Kooistra, G.K. Kanev, O.P. van Linden, R. Leurs, I.J. de Esch, C. de Graaf, KLIFS: a structural kinase-ligand interaction database, Nucleic Acids Res. 44 (D1) (2016) D365–D371, https://doi.org/10.1093/nar/gkv1082.
[69] G.K. Kanev, C. de Graaf, B.A. Westerman, I.J.P. de Esch, A.J. Kooistra, KLIFS: an overhaul after the first 5 years of supporting kinase research, Nucleic Acids Res. (2020) gkaa895, https://doi.org/10.1093/nar/gkaa895.
[70] B. Wienen-Schmidt, D. Schmidt, H.D. Gerber, A. Heine, H. Gohlke, G. Klebe, Surprising non-additivity of methyl groups in drug-kinase interaction, ACS Chem. Biol. 14 (2019) 2585–2594, https://doi.org/10.1021/acschembio.9b00476.
[71] D. Bajusz, G.G. Ferenczy, G.M. Keserű, Structure-based virtual screening approaches in kinase-directed drug discovery, Curr. Top. Med. Chem. 17 (2017) 2235–2259, https://doi.org/10.2174/1568026617666170224121313.
[72] P. Wu, T.E. Nielsen, M.H. Clausen, FDA-approved small-molecule kinase inhibitors, Trends Pharm. Sci. 36 (2015) 422–439, https://doi.org/10.1016/j.tips.2015.04.005.
[73] M.L. Vazquez, N. Kaila, J.W. Strohbach, J.D. Trzupek, M.F. Brown, M. E. Flanagan, M.J. Mitton-Fry, T.A. Johnson, R.E. TenBrink, E.P. Arnold, A. Basak, S.E. Heasley, S. Kwon, J. Langille, M.D. Parikh, S.H. Griffin, J.M. Casavant, B. A. Duclos, A.E. Fenwick, T.M. Harris, S. Han, N. Caspers, M.E. Dowty, X. Yang, M. E. Banker, M. Hegen, P.T. Symanowicz, L. Li, L. Wang, T.H. Lin, J. Jussif, J. D. Clark, J.B. Telliez, R.P. Robinson, R. Unwalla, Identification of N-{cis-3-[Methyl(7H-pyrrolo[2,3-*d*]pyrimidin-4-yl)amino]cyclobutyl}propane-1-sulfonamide (PF-04965842): a selective JAK1 clinical candidate for the treatment of autoimmune diseases, J. Med. Chem. 61 (2018) 1130–1152, https://doi.org/10.1021/acs.jmedchem.7b01598.
[74] M. Nogueira, T. Torres, Janus Kinase inhibitors for the treatment of atopic dermatitis: focus on abrocitinib, baricitinib, and upadacitinib, Dermatol. Pr. Concept 11 (2021), e2021145, https://doi.org/10.5826/dpc.1104a145.
[75] A.M. Shawky, F.A. Almalki, A.N. Abdalla, A.H. Abdelazeem, A.M. Gouda, A comprehensive overview of globally approved JAK inhibitors, Pharmaceutics 14 (2022) 1001, https://doi.org/10.3390/pharmaceutics14051001.
[76] E.D. Deeks, S. Duggan, Abrocitinib: first approval, Drugs 81 (2021) 2149–2157, https://doi.org/10.1007/s40265-021-01638-3.
[77] M. Kalyukina, Y. Yosaatmadja, M.J. Middleditch, A.V. Patterson, J.B. Smaill, C. J. Squire, TAS-120 cancer target binding: defining reactivity and revealing the first fibroblast growth factor receptor1 (FGFR1) irreversible structure, ChemMedChem 14 (2019) 494–500.
[78] L. Goyal, L. Shi, L.Y. Liu, F.F. de la Cruz, J.K. Lennerz, S. Raghavan, I. Leschiner, L. Elagina, G. Siravegna, R.W. Ng, P. Vu, K.C. Patra, S.K. Saha, R.N. Uppot, R. Arellano, S. Reyes, T. Sagara, S. Otsuki, B. Nadres, H.A. Shahzade, I. Dey-Guha, I.J. Fetter, I. Baiev, P. Van Seventer, J.E. Murphy, C.R Ferrone, K.K. Tanabe, V. Deshpande, J.J. Harding, R. Yaeger, R.K. Kelley, A. Bardelli, A.J. Iafrate, W. C. Hahn, C.H. Benes, D.T. Ting, H. Hirai, G. Getz, D. Juric, A.X. Zhu, R. B. Corcoran, N. Bardeesy, TAS-120 overcomes resistance to ATP-competitive FGFR inhibitors in patients with FGFR2 fusion-positive intrahepatic cholangiocarcinoma, Cancer Discov. 9 (2019) 1064–1079, https://doi.org/10.1158/2159-8290.CD-19-0182.
[79] A. Vogel, O. Segatto, A. Stenzinger, A. Saborowski, FGFR2 inhibition in cholangiocarcinoma, Annu Rev. Med. (2022), https://doi.org/10.1146/annurev-med-042921-024707.
[80] F. Meric-Bernstam, R. Bahleda, C. Hierro, M. Sanson, J. Bridgewater, H. T. Arkenau, B. Tran, R.K. Kelley, J.O. Park, M. Javle, Y. He, K.A. Benhadji, L. Goyal, Futibatinib, an irreversible FGFR1-4 inhibitor, in patients with advanced solid tumors harboring FGF/ FGFR aberrations: A phase I dose-expansion study, Cancer Discov. 12 (2022) 402–415, https://doi.org/10.1158/2159-8290.CD-21-0697.
[81] P.W. Manley, L. Barys, S.W. Cowan-Jacob, The specificity of asciminib, a potential treatment for chronic myeloid leukemia, as a myristate-pocket binding ABL inhibitor and analysis of its interactions with mutant forms of BCR-ABL1 kinase, Leuk. Res. 98 (2020), 106458, https://doi.org/10.1016/j.leukres.2020.106458.
[82] A.A. Adzhubei, M.J. Sternberg, A.A. Makarov, Polyproline-II helix in proteins: structure and function, J. Mol. Biol. 425 (2013) 2100–2132.
[83] B.A. Liu, B.W. Engelmann, P.D. Nash, The language of SH2 domain interactions defines phosphotyrosine-mediated signal transduction, FEBS Lett. 586 (2012) 2597–2605.
[84] Z. Songyang, L.C. Cantley, Recognition and specificity in protein tyrosine kinase-mediated signalling, Trends Biochem. Sci. 20 (1995) 470–475, https://doi.org/10.1016/s0968-0004(00)89103-3.
[85] O. Hantschel, G. Superti-Furga, Regulation of the c-Abl and Bcr-Abl tyrosine kinases, Nat. Rev. Mol. Cell Biol. 5 (2004) 33–44, https://doi.org/10.1038/nrm1280.
[86] O. Hantschel, B. Nagar, S. Guettler, J. Kretzschmar, K. Dorey, J. Kuriyan, G. Superti-Furga, A myristoyl/phosphotyrosine switch regulates c-Abl, Cell 112 (2003) 845–857, https://doi.org/10.1016/s0092-8674(03)00191-0.
[87] B. Nagar, O. Hantschel, M.A. Young, K. Scheffzek, D. Veach, W. Bornmann, B. Clarkson, G. Superti-Furga, J. Kuriyan, Structural basis for the autoinhibition of c-Abl tyrosine kinase, Cell 112 (2003) 859–871, https://doi.org/10.1016/s0092-8674(03)00194-6.
[88] C. Arter, L. Trask, S. Ward, S. Yeoh, R. Bayliss, Structural features of the protein kinase domain and targeted binding by small-molecule inhibitors, J. Biol. Chem. 298 (2022), 102247, https://doi.org/10.1016/j.jbc.2022.102247.
[89] J. Yang, N. Campobasso, M.P. Biju, K. Fisher, X.Q. Pan, J. Cottom, S. Galbraith, T. Ho, H. Zhang, X. Hong, P. Ward, G. Hofmann, B. Siegfried, F. Zappacosta, Y. Washio, P. Cao, J. Qu, S. Bertrand, D.Y. Wang, M.S. Head, H. Li, S. Moores, Z. Lai, K. Johanson, G. Burton, C. Erickson-Miller, G. Simpson, P. Tummino, R.

A. Copeland, A. Oliff, Discovery and characterization of a cell-permeable, small-molecule c-Abl kinase activator that binds to the myristoyl binding site, Chem. Biol. 18 (2011) 177–186, https://doi.org/10.1016/j.chembiol.2010.12.013.
[90] J. Schoepfer, W. Jahnke, G. Berellini, S. Buonamici, S. Cotesta, S.W. Cowan-Jacob, S. Dodd, P. Drueckes, D. Fabbro, T. Gabriel, J.M. Groell, R.M. Grotzfeld, A. Q. Hassan, C. Henry, V. Iyer, D. Jones, F. Lombardo, A. Loo, P.W. Manley, X. Pellé, G. Rummel, B. Salem, M. Warmuth, A.A. Wylie, T. Zoller, A.L. Marzinzik, P. Furet, Discovery of asciminib (ABL001), an allosteric inhibitor of the tyrosine kinase activity of BCR-ABL1, J. Med. Chem. 61 (2018) 8120–8135, https://doi.org/10.1021/acs.jmedchem.8b01040.
[91] E.D. Deeks, Asciminib: first approval, Drugs 82 (2022) 219–226, https://doi.org/10.1007/s40265-021-01662-3.
[92] Y.N. Lamb, Pacritinib: First approval, Drugs 82 (2022) 831–838, https://doi.org/10.1007/s40265-022-01718-y.
[93] J. Mascarenhas, Pacritinib for the treatment of patients with myelofibrosis and thrombocytopenia, Expert Rev. Hematol. 15 (2022) 671–684, https://doi.org/10.1080/17474086.2022.2112565.
[94] C.A. Lipinski, F. Lombardo, B.W. Dominy, P.J. Feeney, Experimental and computational approaches to estimate solubility and permeability in drug discovery and development settings, Adv. Drug Deliv. Rev. 46 (2001) 3–26, https://doi.org/10.1016/s0169-409x(00)00129-0.
[95] A.L. Hopkins, C.R. Groom, A. Alex, Ligand efficiency: a useful metric for lead selection, Drug Discov. Today 9 (2004) 430–431, https://doi.org/10.1016/S1359-6446(04)03069-7.
[96] P.D. Leeson, B. Springthorpe, The influence of drug-like concepts on decision-making in medicinal chemistry, Nat. Rev. Drug Discov. 6 (2007) 881–890, https://doi.org/10.1038/nrd2445.
[97] S. Ekins, N.K. Litterman, C.A. Lipinski, B.A. Bunin, Thermodynamic proxies to compensate for biases in drug discovery methods, Pharm. Res. 33 (2016) 194–205, https://doi.org/10.1007/s11095-015-1779-y.
[98] A.L. Hopkins, G.M. Keserü, P.D. Leeson, D.C. Rees, C.H. Reynolds, The role of ligand efficiency metrics in drug discovery, Nat. Rev. Drug Discov. 13 (2014) 105–121, https://doi.org/10.1038/nrd4163.
[99] P.D. Leeson, Molecular inflation, attrition, and the rule of five, Adv. Drug Deliv. Rev. 101 (2016) 22–33, https://doi.org/10.1016/j.addr.2016.01.018.
[100] D.F. Veber, S.R. Johnson, H.Y. Cheng, B.R. Smith, K.W. Ward, K.D. Kopple, Molecular properties that influence the oral bioavailability of drug candidates, J. Med Chem. 45 (2002) 2615–2623, https://doi.org/10.1021/jm020017n.
[101] T.I. Oprea, Property distribution of drug-related chemical databases, J. Comput. Aided Mol. Des. 14 (2000) 251–264, https://doi.org/10.1023/a:1008130001697.
[102] P.D. Leeson, A.P. Bento, A. Gaulton, A. Hersey, E.J. Manners, C.J. Radoux, A. R. Leach, Target-based evaluation of "drug-like" properties and ligand efficiencies, J. Med Chem. 64 (2021) 7210–7230, https://doi.org/10.1021/acs.jmedchem.1c00416.
[103] J.J. Cui, M. McTigue, M. Nambu, M. Tran-Dubé, M. Pairish, H. Shen, L. Jia, H. Cheng, J. Hoffman, P. Le, M. Jalaie, G.H. Goetz, K. Ryan, N. Grodsky, Y. L. Deng, M. Parker, S. Timofeevski, B.W. Murray, S. Yamazaki, S. Aguirre, Q. Li, H. Zou, J. Christensen, Discovery of a novel class of exquisitely selective mesenchymal-epithelial transition factor (c-MET) protein kinase inhibitors and identification of the clinical candidate 2-(4-(1-(quinolin-6-ylmethyl)-1H-[1,2,3]triazolo[4,5-*b*]pyrazin-6-yl)-1H-pyrazol-1-yl)ethanol (PF-04217903) for the treatment of cancer, J. Med Chem. 55 (2012) 8091–8109, https://doi.org/10.1021/jm300967g.
[104] S.H. Bertz, The first general index of molecular complexity, J. Am. Chem. Soc. 1103 (1981) 3559–3601.
[105] J.B. Hendrickson, P. Huang, A.G. Toczko, Molecular complexity: a simplified formula adapted to individual atoms, J. Chem. Inf. Comput. Sci. 27 (1987) 63–67.
[106] T.J. Ritchie, S.J. Macdonald, Physicochemical descriptors of aromatic character and their use in drug discovery, J. Med. Chem. 57 (2014) 7206–7215, https://doi.org/10.1021/jm500515d.
[107] M.K. Bayliss, J. Butler, P.L. Feldman, D.V. Green, P.D. Leeson, M.R. Palovich, A. J. Taylor, Quality guidelines for oral drug candidates: dose, solubility and lipophilicity, Drug Discov. Today 21 (2016) 1719–1727, https://doi.org/10.1016/j.drudis.2016.07.007.
[108] T.I. Oprea, C.G. Bologa, S. Brunak, A. Campbell, G.N. Gan, A. Gaulton, S. M. Gomez, R. Guha, A. Hersey, J. Holmes, A. Jadhav, L.J. Jensen, G.L. Johnson, A. Karlson, A.R. Leach, A. Ma'ayan, A. Malovannaya, S. Mani, S.L. Mathias, M. T. McManus, T.F. Meehan, C. von Mering, D. Muthas, D.T. Nguyen, J. P. Overington, G. Papadatos, J. Qin, C. Reich, B.L. Roth, S.C. Schürer, A. Simeonov, L.A. Sklar, N. Southall, S. Tomita, I. Tudose, O. Ursu, D. Vidovic, A. Waller, D. Westergaard, J.J. Yang, G. Zahoránszky-Köhalmi, Unexplored therapeutic opportunities in the human genome, Nat. Rev. Drug Discov. 17 (2018) 377, https://doi.org/10.1038/nrd.2018.52.
[109] L. Huang, S. Jiang, Y. Shi, Tyrosine kinase inhibitors for solid tumors in the past 20 years (2001-2020), J. Hematol. Oncol. 13 (2020) 143, https://doi.org/10.1186/s13045-020-00977-0.
[110] K. Bechman, M. Yates, J.B. Galloway, The new entries in the therapeutic armamentarium: the small molecule JAK inhibitors, Pharm. Res. 147 (2019), 104392, 10.1016/j.phrs.2019.104392. Corrigendum doi: 10.1016/j.phrs.2020.104634.
[111] Bechman K., Galloway G.B., Winthrop K.L. Small-molecule protein kinase inhibitors and the risk of fungal infections. Curr Fungal Infect Rep. 10.1007/s12281–019-00350-w.
[112] C.I. Wells, H. Al-Ali, D.M. Andrews, C.R.M. Asquith, A.D. Axtman, I. Dikic, D. Ebner, P. Ettmayer, C. Fischer, M. Frederiksen, R.E. Futrell, N.S. Gray, S. B. Hatch, S. Knapp, U. Lücking, M. Michaelides, C.E. Mills, S. Müller, D. Owen, A. Picado, K.S. Saikatendu, M. Schröder, A. Stolz, M. Tellechea, B.J. Turunen, S. Vilar, J. Wang, W.J. Zuercher, T.M. Willson, D.H. Drewry, The kinase chemogenomic set (KCGS): an open science resource for kinase vulnerability identification, Int J. Mol. Sci. 22 (2021) 566, https://doi.org/10.3390/ijms22020566.
[113] J. Choo, G. Heo, C. Pothoulakis, E. Im, Posttranslational modifications as therapeutic targets for intestinal disorders, Pharm. Res. (2021), 105412, https://doi.org/10.1016/j.phrs.2020.105412.
[114] C.C. Ayala-Aguilera, T. Valero, Á. Lorente-Macías, D.J. Baillache, S. Croke, A. Unciti-Broceta, small molecule kinase inhibitor drugs (1995-2021): medical indication, pharmacology, and synthesis, J. Med Chem. 65 (2022) 1047–1131, https://doi.org/10.1021/acs.jmedchem.1c00963.
[115] Z. Xie, X. Yang, Y. Duan, J. Han, C. Liao, Small-molecule kinase inhibitors for the treatment of nononcologic diseases, J. Med. Chem. 64 (2021) 1283–1345.
[116] R. Roskoski Jr., Blockade of mutant RAS oncogenic signaling with a special emphasis on KRAS, Pharm. Res. 172 (2021), 105806, https://doi.org/10.1016/j.phrs.2021.105806.
[117] A. Cichońska, B. Ravikumar, R.J. Allaway, F. Wan, S. Park, O. Isayev, S. Li, M. Mason, A. Lamb, Z. Tanoli, M. Jeon, S. Kim, M. Popova, S. Capuzzi, J. Zeng, K. Dang, G. Koytiger, J. Kang, C.I. Wells, T.M. Willson, IDG-DREAM Drug-Kinase Binding Prediction Challenge Consortium, T.I. Oprea, A. Schlessinger, D. H. Drewry, G. Stolovitzky, K. Wennerberg, J. Guinney, T. Aittokallio, Crowdsourced mapping of unexplored target space of kinase inhibitors, Nat. Commun. 12 (2021) 3307, https://doi.org/10.1038/s41467-021-23165-1.
[118] H.Y. Min, H.Y. Lee, Molecular targeted therapy for anticancer treatment, Exp. Mol. Med. (2022), https://doi.org/10.1038/s12276-022-00864-3.
[119] X. Lu, J.B. Smaill, K. Ding, New promise and opportunities for allosteric kinase inhibitors, Angew. Chem. Int Ed. Engl. 59 (2020) 13764–13776, https://doi.org/10.1002/anie.201914525.
[120] K. Sasaki, S.S. Strom, S. O'Brien, E. Jabbour, F. Ravandi, M. Konopleva, G. Borthakur, N. Pemmaraju, N. Daver, P. Jain, S. Pierce, H. Kantarjian, J. E. Cortes, Relative survival in patients with chronic-phase chronic myeloid leukaemia in the tyrosine-kinase inhibitor era: analysis of patient data from six prospective clinical trials, Lancet Haematol. 2 (2015) e186–e193, https://doi.org/10.1016/S2352-3026(15)00048-4.
[121] H.M. Kantarjian, N. Jain, G. Garcia-Manero, M.A. Welch, F. Ravandi, W. G. Wierda, E.J. Jabbour, The cure of leukemia through the optimist's prism, Cancer 128 (2022) 240–259, https://doi.org/10.1002/cncr.33933.
[122] E. Jabbour, H. Kantarjian, J. Cortes, Use of second- and third-generation tyrosine kinase inhibitors in the treatment of chronic myeloid leukemia: an evolving treatment paradigm, Clin. Lymphoma Myeloma Leuk. 15 (2015) 323–334, https://doi.org/10.1016/j.clml.2015.03.006.
[123] J. Cortes, C. Pavlovsky, S. Saußele, Chronic myeloid leukemia, Lancet 398 (2021) 1914–1926, https://doi.org/10.1016/S0140-6736(21)01204-6.
[124] F.G. Haddad, K. Sasaki, G.C. Issa, G. Garcia-Manero, F. Ravandi, T. Kadia, J. Cortes, M. Konopleva, N. Pemmaraju, Y. Alvarado, M. Yilmaz, G. Borthakur, C. DiNardo, N. Jain, N. Daver, N.J. Short, E. Jabbour, H. Kantarjian, Treatment-free remission in patients with chronic myeloid leukemia following the discontinuation of tyrosine kinase inhibitors, Am. J. Hematol. 97 (2022) 856–864, https://doi.org/10.1002/ajh.26550.
[125] R. Roskoski Jr., Guidelines for preparing color figures for everyone including the colorblind, in: Pharmacol Res., 119, 2017, pp. 240–241.